


Handbook
for
Generic Photonic IC Design

Editors: Meint Smit and Xaveer Leijtens

4-4-2026

 *Handbook for generic photonic IC design*, by the *Photonic Integration group*, Technische Universiteit Eindhoven, is licensed under a Creative Commons “Attribution-NonCommercial-NoDerivatives 4.0 International” license.

We traced the ownership of all figures used as far as we could. However, if you are a copyright owner and believe we used your work without permission, please contact us at coordinator@jeppix.eu.

Chapter 1

An introduction to InP-based generic integration technology

MEINT SMIT ET AL.

Photonic integrated circuits (PICs) are the way to make advanced photonic systems or subsystems cheap if they are fabricated in large volumes. They are much more compact and robust than their discrete counterparts, but their development costs are high, which has restricted their application to a few niche markets where their superior properties outweighed their high cost. They are rapidly gaining importance in high-speed telecommunication systems using advanced modulation formats, where integration offers large advantages. However, in other application fields their high development costs are still a barrier for broad application.

An important development is the emergence of a novel approach in design and manufacturing, which reduces the R&D and prototyping costs and the throughput time of PICs by more than an order of magnitude. It brings the application of PICs that integrate complex and advanced photonic functionality on a single chip within reach for a large number of small and larger companies and it is initiating a breakthrough in the application of Photonic ICs. In this introductory chapter we will explain the concept of generic photonic integration technology using the technology developed by the COBRA¹ research institute of TU Eindhoven, as an example. The chapter is a slightly adapted version of an introductory paper published in the *Journal of Semiconductor Science and Technology*²[1]. The following chapters are divided in three parts.

In Part I the Physics and Technology is explained that is required for understanding the chapters on building blocks. Chapter 2 explains the theory of waveguides, chapter 3 explains the semiconductor physics required for understanding lasers, detectors,

¹Since 2015 COBRA has been integrated in the Institute of Photonic Integration (IPI) of TU Eindhoven and since 2021 in the Eindhoven Hendrik Casimir Institute (EHCI).

²Author list: Meint Smit, Xaveer Leijtens, Huub Ambrosius, Erwin Bente, Jos van der Tol, Barry Smalbrugge, Tjibbe de Vries, Erik-Jan Geluk, Jeroen Bolk, Rene van Veldhoven, Luc Augustin, Peter Thijs, Domenico D'Agostino, Hadi Rabbani, Katarzyna Lawniczuk, Stanislaw Stopinski, Saeed Tahvili, Antonio Corradi, Emil Kleijn, Dzmityr Dzibrou, Manuela Felicetti, Elton Bitincka, Valentina Moskalenko, Jing Zhao, Rui Santos, Giovanni Gilardi, Weiming Yao, Kevin Williams, Patty Stabile, Piet Kuindersma, Josselin Pello, Srivathsa Bhat, Yuqing Jiao, Dominik Heiss, Gunther Roelkens, Mike Wale, Paul Firth, Francisco Soares, Norbert Grote, Martin Schell, Hélène Debregeas, Mohand Achouche, Jean-Louis Gentner, Arjen Bakker, Twan Korthorst, Dominic Gallagher, Andrew Dabbs, Andrea Melloni, Francesco Morichetti, Daniele Melati, Adrian Wonfor, Richard Penty, Ronald Broeke, Bob Musk and Dave Robbins.

modulators and optical amplifiers. Chapter 4 explains the fabrication technology of Photonic ICs. Chapter 5 explains some methods for component and circuit design and simulation, and Chapter 6 gives an overview of some of the design tools and their capabilities. Chapter 7 discusses some methods for characterizing PICs and Chapter 8 for assembling and packaging the PICs and testing their performance.

In Part II the basic building blocks in InP-based Photonic IC design are explained: passive waveguides (chapter 9), waveguide junctions (chapter 10), polarisation converters (chapter 11), waveguide gratings (chapter 12), elements for coupling light in or out of the chip (chapter 13), optical amplifiers (chapter 14), detectors (chapter 15), saturable absorbers (chapter 16), modulators (chapter 17) and on-chip rf-connections and components (chapter 18).

In Part III more complex components, composed of several basic building blocks, are described: junctions between different types of waveguides (chapter 21), devices based on multi-mode interference (MMI couplers, chapter 19), Y-junctions (chapter 22), directional couplers (chapter 20), star couplers (chapter 23), optical phased arrays (chapter 24), arrayed waveguide grating (de)multiplexers and routers (chapter 25), Mach-Zehnder modulators (chapter 26), components for polarisation handling (chapter 27), resonators, which are important elements in lasers and filters (chapter 28), lasers (chapter 29).

In Part IV some worked examples of Photonic IC design are discussed (chapter 30) and the book is concluded with a chapter about future developments (chapter 31).

1.1 Background

1.1.1 History of Photonic Integration

After its first appearance in the published literature over forty years ago [2], it was believed that microphotonic integration would take a similar development path to that followed by microelectronic integration. In his review paper of 1977 Tien [3] mentioned as one of the major goals of microphotonic integration or “Integrated Optics” as it was called at the time: “*the integration of a large number of optical devices on a small substrate, so forming an optical circuit reminiscent of the integrated circuit in microelectronics*”. In the following years a number of chips of increasing complexity were reported. Figure 1.1 shows the complexity development measured as the number of components integrated on a single chip³. The underlying data is summarized in Table 1.1 and briefly described below.

Early examples of complex InP-based photonic integrated circuits (PICs) are a WDM source by Koren [4], integrating three lasers consisting of a semiconductor optical amplifier (SOA) and a tunable Bragg Grating Reflector, with a power combiner and a booster SOA on a single chip; a grating-based receiver by Cremer [5], integrating an Echelle grating demultiplexer with more than 30 detectors; a 4×4 cross-bar switch by Duthie [6], integrating 16 reverse- $\Delta\beta$ switches; a switch array by Gustavsson [7], integrating 24 SOA gate switches with 24 1×2 couplers; and a polarization diversity heterodyne receiver by Kaiser [8], integrating a DBR-type local oscillator laser with polarization

³Several metrics have been proposed for measuring chip complexity. We use a simple but coarse approach in which we count the number of basic components like AWGs, MMIs, SOAs, detectors and modulators. It does not count for the fact that a DFB laser is more complex than an MMI coupler, for example, so a higher number of components does not always mean a more complex chip. Further, we count only components that are essential for the PIC-functionality (e.g. no spare components that are not essential for the functionality).

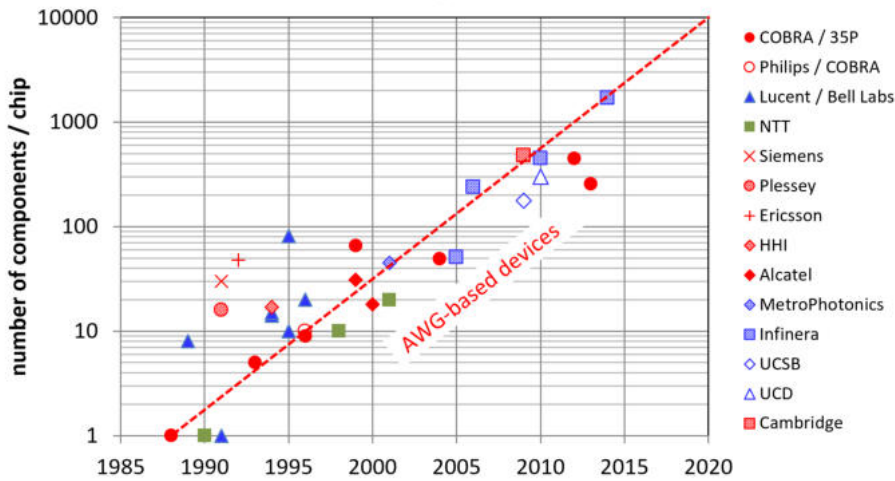


Figure 1.1: Development of chip complexity measured as the number of components per chip.

mode splitters, polarization mode filters, 3 dB combiners, detector diodes in balanced configuration, junction FETs and load resistors.

The highest complexities so far have been reported in AWG-based PICs. It started with the publication of the first AWG by Smit [9] in 1988, followed by Takahashi [10] and Dragone [11]. After the invention of the AWG a number of AWG-based devices with increasing circuit complexity were reported: WDM receivers with 5–10 components by Amersfoort [12], Zirngibl [13] and Steenbergen [14]; WDM lasers with 10–20 components by Zirngibl [15, 16] and Staring [17]; WDM channel selectors with 10–20 components by Zirngibl [18], Ishii [19], Menezes (1999) [20], Mestric [21] and Kikuchi [22] and a crossconnect chip with 66 components by Herben [23]. A special device is the WDM-receiver with integrated pre-amplifiers by Chandrasekhar [24] which counts 81 components, most of them electronic (transistors and resistors).

Figure 1.2 illustrates two of these WDM devices: a WDM receiver with 9 components and a WDM crossconnect with 66 components.

The new century brought a significant increase in complexity: WDM receiver and transmitter chips with 44–51 components by Tolstikhin [27], ThreeFivePhotonics [25] and Infinera [28]. Shortly after, in 2006, Infinera published a 40-channel WDM transmitter with 241 components [29]. Figure 1.2c illustrates the 40-channel WDM monitor chip with 49 components developed by Three-Five Photonics and Figure 1.2d an 8×8 wavelength router chip with 175 components reported by Nicholes in 2009 [26]. In the same year Wang [30] reported a 16×16 SOA switch matrix with 480 components, and one year later Soares [31] a 100-channel Arbitrary Waveform Generator with more than 300 components. The latter device also contains 400 phase shifters for reducing the high crosstalk level in the very large AWG which is used to separate 100 wavelength channels. Two other PICs with more than 400 components have been reported by Corzine (Infinera) and Stabile (COBRA) [32, 33]. Table 1.1 gives an overview of the devices mentioned. An excellent overview of High Performance InP-Based Photonic ICs is given by Coldren [36].

In microelectronics there is a clear exponential development in the number of transistors per chip, which has been doubling every two years on average during the last four decades. This phenomenon is known as Moore's law [37, 38]. Figure 1.1 reveals a

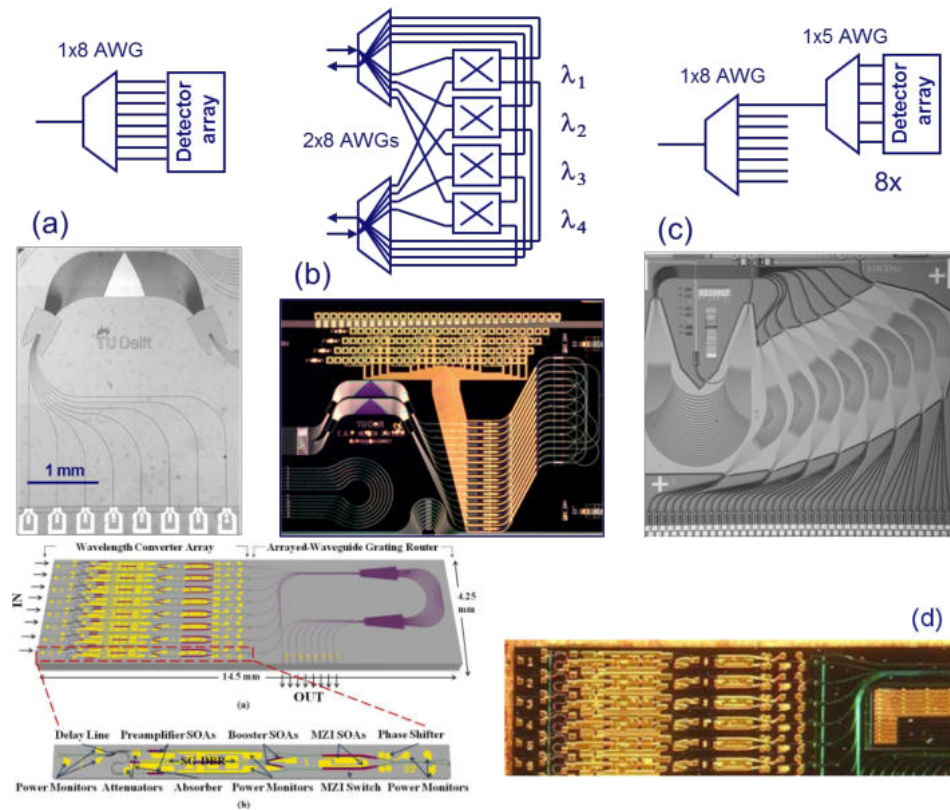


Figure 1.2: Examples of Photonic ICs: a) a WDM receiver consisting of an AWG integrated with 8 detector diodes [14]; b) a 4-channel 2×2 WDM crossconnect integrating 2 AWGs with 16 Mach-Zehnder Interferometer switches in dilated configuration (66 components in total); c) a 40-channel WDM monitor chip integrating 9 AWGs and 40 detector diodes [25]; d) an 8×8 channel wavelength router, integrating 8 wavelength converter circuits with an 8×8 AWG, with over 175 components [26].

Year	#Comp	Short title	1 st author	Institute	Ref
1988	1	AWG	Smit	COBRA	[9]
1989	8	WDM source	Koren	Bell Labs	[4]
1990	1	AWG	Takahashi	NTT	[10]
1991	30	Grating Spectrograph	Cremer	Siemens	[5]
1991	1	AWG	Dragone	Bell Labs	[11]
1992	48	Switch Array	Gustavsson	Ericsson	[7]
1993	5	WDM receiver	Amersfoort	COBRA	[12]
1994	17	Heterodyne receiver	Kaiser	HHI	[8]
1994	14	WDM laser	Zirngibl	Bell Labs	[15]
1994	15	WDM channel selector	Zirngibl	Bell Labs	[18]
1995	10	WDM receiver	Zirngibl	Bell Labs	[13]
1995	81	WDM receiver & preamp	Chandrasekhar	Bell Labs	[24]
1996	9	WDM receiver	Steenbergen	COBRA	[14]
1996	20	WDM laser	Zirngibl	Lucent	[16]
1996	10	WDM laser	Staring	Philips	[17]
1998	10	WDM channel selector	Ishii	NTT	[19]
1999	66	WDM crossconnect	Herben	COBRA	[23]
1999	31	WDM laser	Menoza	Alcatel	[20]
2000	18	WDM channel selector	Mestric	Alcatel	[21]
2001	20	WDM channel selector	Kikuchi	NTT	[22]
2003	45	WDM receiver	Tolstikhin	MetroPhotonics	[27]
2004	49	WDM receiver	35 Photonics	35Photonics	[25]
2005	51	WDM transmitter	Nagarajan	Infinera	[28]
2006	240	WDM transmitter	Kato	Infinera	[29]
2009	177	Tunable WDM router	Nicholes	UCSB	[26]
2009	480	16 × 16 SOA switch	Wang	UCAM	[30]
2010	302	Arb. Waveform Generator	Soares	UCD	[31]
2010	450	PM-DQPSK WDM transm.	Corzine	Infinera	[32]
2012	480	16 × 16 switch	Stabile	COBRA	[33]
2013	256	8 × 8 wavelength switch	Stabile	COBRA	[34]
					[35]

Table 1.1: Development of chip complexity measured as the number of components (#Comp) per chip.

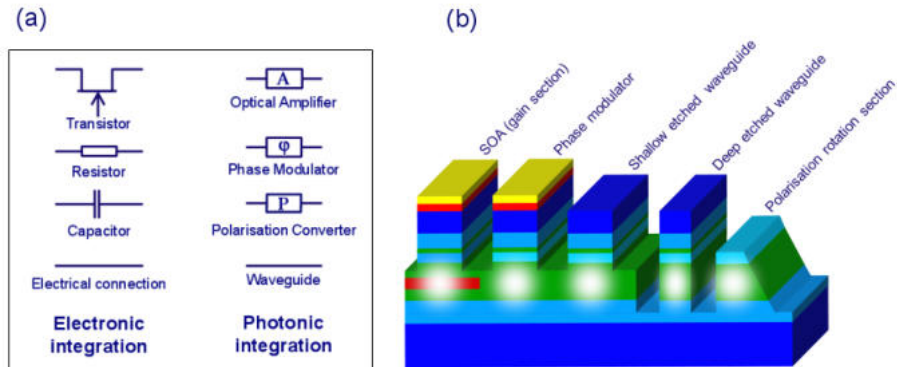


Figure 1.3: a) Basic Building Blocks in generic electronic and photonic integration processes. b) Schematic cross section of the basic building blocks in a generic photonic integration process.

similar development in microphotonics, albeit in an early stage and with a much larger scatter than its microelectronic counterpart. If we restrict ourselves to devices based on AWGs, with a more or less comparable technology (AWGs with integrated amplifiers and/or detectors) most of the outliers disappear, however, which suggests that photonic integration is taking a similar development path to microelectronics, probably driven by the same improvements in process technology and equipment.

1.1.2 Generic Photonic Integration Technology

Despite similarities in the development of chip complexity there is a marked difference between today's microphotonics and microelectronics, and that is in the R&D methodology followed. In microphotonics most integration technologies are developed and optimized for a specific application. As a result we have almost as many technologies as applications, most of them very similar, but sufficiently different to prevent easy transfer of a design from one fab to another. Owing to this huge fragmentation, the market for many of these application-specific technologies is too small to justify their further development into a low-cost industrial volume manufacturing process. And as a result the chip costs remain too high to find wide application.

This is quite different from microelectronics where a huge market is served by a small set of integration processes (most of them CMOS processes). In these processes a broad range of functionalities can be realised from a small set of basic building blocks, like transistors, resistors, capacitors and interconnection tracks. By connecting these building blocks in different numbers and topologies we can realize a huge variety of circuits and systems, with complexities ranging from a few hundred up to over a billion transistors. We call such a process, in which a broad range of functionalities can be synthesized from a small set of basic building blocks, a *generic integration process*.

In photonics we can do something similar, as illustrated in Figure 1.3a. An integration process with building blocks for controlling the basic properties of light: the amplitude, the phase and the polarization, can support a broad range of functionalities. Figure 1.3b shows a schematic picture of five different components integrated in a single generic integration process on an InP substrate. The example is taken from the process of the former COBRA research institute of TU Eindhoven, which is now called EHCI (Eindhoven Hendrik Casimir Institute). The green layer is the waveguide layer that carries the optical waveguide modes (indicated by a white spot); the dark red layer the

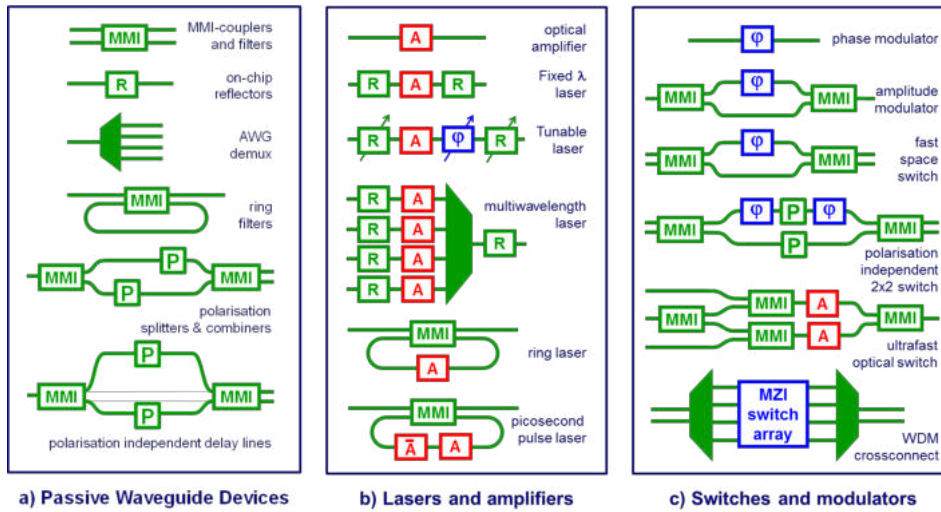


Figure 1.4: Examples of the functionalities that can be realized with (a) passive waveguide devices alone, or in combination with (b) optical amplifiers and (c) phase modulators.

optically active gain medium. With a good waveguide structure we can make interconnections, but also passive components like couplers, filters and demultiplexers. With optical amplifiers (SOA: Semiconductor Optical Amplifier), phase modulators and polarization converters, for manipulating the amplitude, the phase and the polarization of the light, the technology can support a broad range of functionalities, as illustrated in Figure 1.4.

Figure 1.4a shows a few components that we can make with passive waveguides. The most important ones are MMI-couplers and AWG-demultiplexers. With deep-etched strong-confinement waveguides we can make MMI-reflectors and compact ring filters. Another important building block that we can make in a passive waveguide is a polarization converter. By placing it appropriately in a Mach-Zehnder Interferometer (MZI) we can make polarization splitters and combiners, and by placing it halfway a polarization dependent component, the response of this component becomes polarization independent.

Semiconductor Optical Amplifiers in combination with passive devices offer a broad range of functionalities, as illustrated in Figure 1.4b: Fabry-Perot lasers, multiwavelength lasers, ring lasers and, when used in combination with a wavelength tunable reflector, also tunable lasers. By using a short SOA section in reverse bias as a Saturable Absorber we can make picosecond pulse lasers. And a SOA in reverse bias can also be used as a detector.

Figure 1.4c illustrates some of the functionalities that we can make by combining phase modulators with passive devices: amplitude modulators, space switches, wavelength selective switches, such as WDM crossconnects and add-drop multiplexers. And by making use of the non-linear properties of SOAs integrated in an MZI we can make ultrafast switches.

An advantage of generic integration technologies is that because they serve many different applications, they justify the investments in developing the technology for a very high performance and reliability at the level of the building blocks. This will make circuits realised in such a technology highly competitive. A single generic process will not

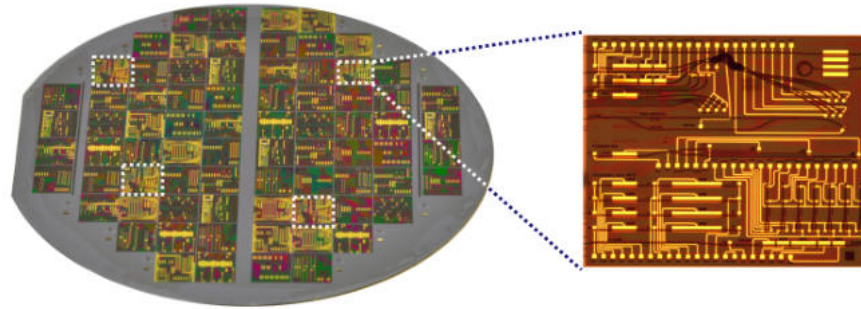


Figure 1.5: Example of a Multi-Project Wafer (MPW) realised in the COBRA process, which is since 2014 offered commercially by SMART Photonics. The wafer contains a large number of cells with different ASPICs. The wafer has 52 cells in the usable wafer area. Each ASPIC is copied at four different locations on the wafer, so that we have room for 12 users and one test cell, which is used for wafer validation. The figure shows one cell (a test cell) and its position on the wafer. In this way, each user will receive four copies of his chip per wafer in the MPW batch. SMART Photonics usually runs two wafers in a batch.

be suited to all applications, of course. Just like in microelectronics we will need a few different generic technologies, optimized for different kinds of applications. But the number of generic technologies can be small, much smaller than the variety in today's technologies.

Further, in a standardized technology we can develop design libraries and a related software infrastructure for components or subcircuits that are used by many designers. This leads to a significant reduction of the design time and an increase in the design accuracy, so that fewer design cycles will be necessary to arrive at a required performance.

All this brings a fundamental change in the business model of photonics and allows commercial and academic groups to co-operate and move forward rather than forever reinventing the wheel.

1.1.3 Multi-Project Wafer Runs

An important advantage of generic integration technology is that a number of different designs can be combined on the same wafer, because they all use the same fabrication process. Such a wafer is called a Multi-Project Wafer (MPW). And the Photonic ICs fabricated in such an MPW run are called ASPICs: Application Specific Photonic ICs, the photonic equivalent of an ASIC. ASPICs are application-specific PICs, realised in a standardized generic process. Figure 1.5 illustrates how a number of designs are combined on a single wafer. In this example there are 12 different designs; each design is repeated four times. So from each wafer in an MPW batch, the designer will receive four chips. This approach leads to a large reduction of the research and development costs. In the development stage often a few design and fabrication cycles are necessary to arrive at the required performance. Usually a few chips out of the wafer are sufficient for testing the design in this stage. By combining a number of designs on a single wafer every designer gets a few chips and the costs of the run can be shared by all participants in the MPW-run. This will lead to a more-than-ten-fold reduction of

the costs of a design run.

1.1.4 Generic Foundry Model

The generic integration approach will lead to a large cost reduction by developing different products in a single or a few highly standardized processes. However, if the owner of the process does not provide access to external users the number of companies that can take advantage of this approach remains restricted. The corner stone of the generic foundry model is, therefore, the generic foundry: a chip manufacturer that provides open access to its generic integration process(es). In silicon microelectronics a number of chip manufacturers are providing such foundry access. In Photonics the generic foundry model is new.

The COBRA research institute of TU Eindhoven has been pioneering generic photonic integration technology since the beginning of the century [39]. The generic approach gained momentum in the European Network of Excellence ePIXnet [40], in which more than 63 research groups active in the field of photonic integration were cooperating in the period from 2004-2009 on a number of photonic integration technologies. InP-based generic photonic integration technology has been explored in a number of European and national projects⁴. Access to InP-based generic foundry processes is organized by the JePPIX platform [46], in which Europe's key players in the field of InP-based photonic integration technology are cooperating. A more detailed description of the InP-based generic foundry approach is given in Smit et al. [47]. At present (semi-) commercial access to InP-based generic foundry processes is offered by two chip manufacturers: the Fraunhofer Heinrich Hertz Institut in Berlin and the COBRA spinoff company SMART Photonics, located in Eindhoven, the Netherlands, which is commercialising the COBRA process.

Figure 1.6 gives a (strongly simplified) explanation how the entry costs are reduced by the introduction of the generic foundry approach. In a vertical integrated fab model the component manufacturer owns the cleanroom facilities. The costs of a well-equipped cleanroom fab for fabrication of Photonic ICs are in the order of one or even a few hundred million Euros (or dollars) for advanced fabs. As shown in Figure 1.6 chip volumes in excess of 10 million mm^2 (2500 3" wafers) are required to bring the investment cost per chip below 10 €/mm². A chip with moderate complexity measures 10-30 mm^2 , so at this price level about one million chips are required for return of investment. Such investments are only affordable for market-dominant, top-tier technology companies.

A few cleanroom owners provide access to fabless customers in order to share the burden of the cleanroom operational expenditure. In this way a fabless customer can avoid the huge investment in a fab and restrict investment to just the development costs of a specific integration process for a specific PIC. We call this model the custom foundry model: the foundry develops application-specific processes for customized PICs. For PICs of moderate complexity the process development costs, including process qualification, are in the order of a million up to a few million Euros and the level of 10 €/mm² is reached at volumes of a few times 10,000 chips (the second curve in Figure 1.6 labeled custom). These are still significant volumes and the investment costs in combination with the risk are prohibitive for most small and medium enterprises (SMEs).

A dramatic further cost reduction can be achieved if the chip design is based on a generic (standardized) integration process, the development costs of which can be

⁴The FP7 European projects EuroPIC [41] and PARADIGM [42], and the Dutch national projects MEMPHIS [43], IOP Photonic Devices [44] and STW GTIP: Generic Technologies in Integrated Photonics [45]

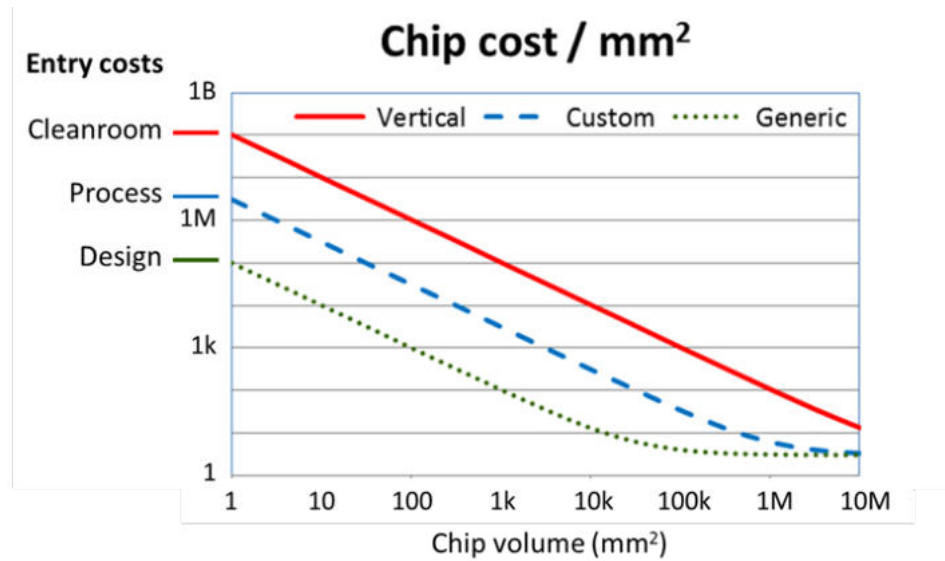


Figure 1.6: The dependence of chip costs on the production volume for three different manufacturing models: a vertical integrated fab model, a custom foundry model and a generic foundry model.

shared by many users. Then the entry costs are mainly restricted to design costs, which can be in the order of 100 k€. The design costs can be reduced even further by development of dedicated Process Design Kits with component libraries that contain the mask layout and accurate models of the building blocks in the foundry platform. This will lead to both a reduction of the design time and the number of design cycles required to arrive at the required performance. In this approach, the cost level of 10 €/mm² can already be reached at volumes of 1000 chips (the third curve in Figure 1.6 labeled generic). It will make entry costs for development of Photonic ICs affordable for most SMEs. We expect, as a consequence, that the introduction of the generic model will lead to a rapid expansion in the application of Photonic ICs.

1.2 Generic Integration Process

There are many kinds of application-specific integration technologies, but also for the more generic technologies there is a large freedom in integration concepts, and different foundries will have different integration technologies, even if they are functionally equivalent. In this chapter we will explain the basics of a generic photonic integration process using the process developed by the COBRA institute of TU Eindhoven as a representative example; it was the first generic process that offered an MPW service and most of the process and building block information is already in the public domain.

The integration process can roughly be subdivided into four process modules, which are illustrated in Figure 1.8 and will be described below in broad outline. We will also indicate some planned developments at the JePPIX Technology Center, in which the JePPIX partners are cooperating on development of novel foundry platform capabilities. Chapter 5 presents a more detailed description.

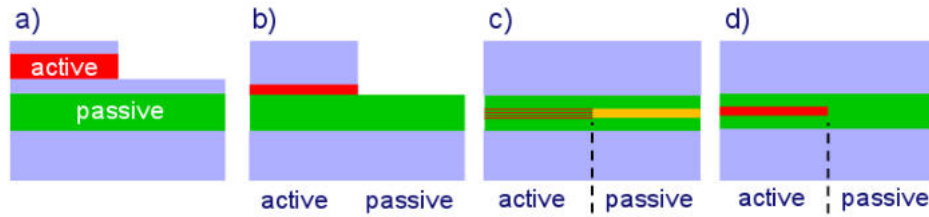


Figure 1.7: Four active-passive integration schemes: a) vertical twin-guide integration, b) vertical single guide integration, c) quantum well intermixing and selective area growth), d) butt-joint integration.

1.2.1 Epitaxial Growth

For the integration of active (amplifier) and passive (transparent waveguide) materials a number of integration schemes have been reported, which can be divided into single and multistep epitaxial growth processes. Epitaxy refers to a type of crystal growth where one layer of crystalline material is deposited on a substrate, which is itself a crystal. This process ensures that the new layer follows the crystallographic orientation of the underlying substrate, resulting in a high-quality crystalline structure.

Epitaxy

Single step epitaxial processes In single-step processes the full layer stack, including active and passive layers is grown in one single epitaxial step and the transparent waveguide sections are created afterwards by locally removing the active layers, as shown in Figure 1.7a and b. Figure 1.7a shows an active waveguide on top of a passive waveguide. In this approach special structures, e.g. vertical tapers, are required for coupling the light smoothly from the active to the passive waveguide and vice versa. A detailed description of a vertical integration approach is given in Menon [48] and Tolstikhin [49]. In Figure 1.7b there is only one (composite) waveguide, which includes the active layer. So no vertical coupling is needed, but at the expense of a discontinuity between the active and the passive waveguide section which causes coupling loss and reflection. The discontinuity can be reduced by applying a taper in the active layer or by covering the structure with an InP cladding layer, but this requires an additional growth step.

Figure 1.7c illustrates another single-step integration method: quantum well intermixing. Here the active layer consists of a number of quantum wells. The active layer can be made passive by capping it with a material which generates vacancies in the semiconductor crystal that diffuse to the active layer when the wafer is heated. These vacancies cause the quantum well atomic species to intermix with those of the barrier layers between them which lead to an increase of the effective bandgap. Intermixing can increase the band gap wavelength of the active material by more than 100 nm, so that it becomes fully transparent. But also intermediate values are possible, e.g. for use in electro-absorption modulators. A detailed description is given by Skogen [50]. One of the disadvantages of this method is that the dopant concentrations in the active and the passive regions are the same, which causes high losses in the transparent regions. This problem can be solved by introducing an additional epitaxial step for growing an undoped cladding layer on the transparent waveguide section (blanket growth).

Single step processes are simple from an epitaxial point of view, but efficient and well controlled coupling between the active and the passive parts introduces additional complexity in the form of taper structures and/or additional growth steps. Figure 1.7d

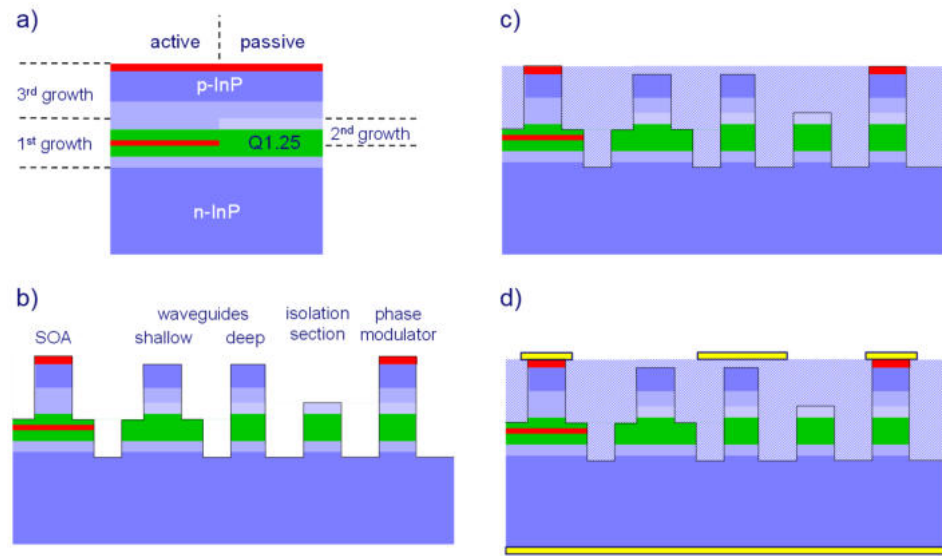


Figure 1.8: Cross section of the wafer structure after the four process modules: a) epitaxial growth, b) waveguide etching, c) passivation and planarization, d) contacting and interconnect metallization.

illustrates the most frequently applied approach: butt-joint integration. Here the active and passive waveguide structures are created in different growth steps, thus providing a large flexibility in the epitaxial layer structure and in the doping levels. In the past the additional growth steps could cause serious yield problems, however, with modern epitaxial technology this is no longer an issue.

Multistep epitaxial growth processes In the COBRA generic process, which is since 2014 commercially offered by SMART Photonics, a three step epitaxial process is used to obtain the structure depicted schematically in Figure 1.7d, and in more detail in Figure 1.8a.

In a first growth step the active layer stack is grown including the lower part of the p-doped cladding. Next the active regions are masked and the exposed area is etched away. In a second selective area regrowth step the etched-away part is replaced with a transparent waveguide stack, up to the same level as the first growth. In the transparent part the cladding layer is not doped in order to avoid absorption loss incurred by the p-dopant. In a third growth step the whole structure is covered with a p-doped cladding layer. If the regrowth process conditions are properly tuned the regrown wafer has a smooth surface and a smooth connection with low reflectivity between the active and the passive waveguide. Tapered and tilted interfaces are beneficial for further reduction of optical losses and reflections.

The process of Fraunhofer HHI differs slightly from this scheme: it uses a semi-insulating (Fe-doped) substrate which leads to better rf-capabilities and enables electrical isolation of individual devices as required for example in balanced detectors. In the following paragraphs we discuss a number of process enhancements that are presently being investigated.

Reduction of waveguide loss In the present integration scheme, the p-doped top cladding, which is required for electrical connection to the active components, introduces an additional waveguide propagation loss of the order of 2 dB/cm for an optimized layer stack design. In larger PICs, which may have several centimetres of waveguide length, this introduces high losses. This loss contribution can be removed by restricting the p-doped cladding layer to the active regions, thus having no p-dopant in the transparent waveguide sections. Losses in the undoped regions are below 1 dB/cm, and the active regions are usually so short that the additional loss contribution due to the p-dopant is a few tenths of a dB at most. A locally undoped cladding layer can be realized by an additional growth step for the transparent waveguide sections or by incorporating the dopant only at the active regions by diffusion through a mask.

Improving rf-performance An important improvement of the performance can be obtained by fabricating the whole circuit on a Semi-Insulating (SI) substrate instead of an n-type substrate, as is presently already done by HHI for its high-speed receiver process. Moving from n-type to SI-substrate requires a redesign of the process, in order to replace the common n-contact at the backside of the wafer by lateral n-contacts which can be accessed from the top of the wafer. An SI-based process brings two advantages. The removal of the conductive n-type ground plane allows for higher speed operation. Both detectors and modulators on SI substrates can operate at frequencies beyond 40 GHz. Further, the n-contact layers of different components can be separated, which allows for integration of balanced photodetectors, where the p-contact from one diode is connected to the n-contact of the other.

Free choice of bandgap Another important extension of the platform capability is to allow a free choice of the bandgap of the active material. At present the same platform process can be applied to source wafers with gain sections containing different gain materials, e.g. bulk, Quantum Well or Quantum Dot layers, but only a limited number of vertical structures can be realized on the same wafer (typically 2 or 3). Hence, in MPW runs a choice has to be made which applies to all participants in that run, there is no flexibility within one chip or wafer.

A process offering more flexibility in bandgap properties is selective area growth (SAG). Here the growth rate in the active regions is enhanced by masking the area besides the active region. During MOVPE growth, species migrate from the masked areas to the unmasked areas where the growth rate becomes higher. If the waveguide consists of an MQW stack the wells in the active region will become thicker and this will lead to a reduction in the bandgap. The reduction can be controlled by controlling the growth enhancement via the width of the mask and the gap between the masked regions. In this way each active region can be controlled individually over a bandgap range as wide as 100 nm [51]. Because the bandgap changes are caused by a diffusion process the connection between regions with different bandgap will be smooth. In order to prevent the variations in layer thickness getting too large the SAG step is usually restricted to the active layer and the cladding layer is grown in an unmasked step. SAG thus requires multiple growth steps.

In this way a whole range of vertical structures can be designed on the same MPW which gives the designer a large degree of freedom in design of active layer properties. Firstly, the vertical structures can be optimised for multiple functionalities on the same wafer: lasers, semiconductor amplifiers, electro-absorption modulators, phase modulators, passive waveguides, etc. Secondly, the layer stacks can be optimized for each operating wavelength. For example in a WDM multiwavelength PIC transmitter, each

laser and each electro-absorption modulator can be optimized individually for each wavelength channel.

1.2.2 Waveguide Etching

The second process module is the waveguide etching. In the COBRA process four etch steps are used for creating four different etch levels, as shown in Figure 1.8b. The deepest level stretches into the substrate and is used in the deep etched waveguides, in deep-etched phase modulators and detector sections (reverse biased SOA sections), and for providing high index contrast. The deep etched waveguides are used where high contrast is essential, e.g. in small-radius bends and in compact MMI-couplers, MMI-reflectors and AWG-(de)multiplexers.

The shallow etch level is used for defining shallow etched waveguides and amplifier sections, where etching through the active regions would cause increased surface recombination. Shallow waveguides show lower propagation losses due to reduced sidewall scattering; they are used for low loss interconnections.

A third etch level is applied for providing electrical isolation between different active components. The isolation is achieved by removing the highly conductive p-doped top cladding layer, down to the low-doped cladding layer just above the waveguide layer. Further, as shown in Figure 3b, this level is used in the polarization rotation sections.

The fourth and shallowest etch step is used for removing the heavily p-doped ternary (InGaAs) contact layer from the passive waveguides, where it contributes to the waveguide losses. Further, after planarization, it allows for routing electrical interconnections across the waveguides, as shown in Figure 1.8d. This is important because it allows routing of the electrical connections to the edge of the chip.

DUV Lithography The quality of the waveguides and the components based on them, such as AWGs and MMI-couplers, is strongly dependent on the quality of the lithography and the etching process. The JePPIX Technology Center has access to a 193 nm DUV scanner (ASML PAS1550/1100) with a resolution down to 90 nm. The machine has been adapted by ASML for handling 3" and 4" InP-wafers. Resolution of this machine is three times better than today's best optical lithography tools for InP-wafers (I-line steppers), which have a resolution of 250 nm.

Such an increase in resolution leads to a large increase in process performance and platform capabilities. An important advantage is that DBR and DFB gratings can be printed with fast optical lithography instead of E-beam lithography or holography. But there are more advantages. The insertion losses of AWGs will reduce from a few dB to less than 1 dB by reducing the closure of the gaps between the array waveguides. With the improved resolution the control of critical dimensions in MMI couplers and polarization converters will become much better allowing more accurate specification of device performance and leading to higher yield. Also, it can be expected that the waveguide propagation losses will become lower due to smoother waveguide edges.

The very thin photoresists that are used for 193 nm DUV lithography are not suited as a mask for etching thick layers and do not tolerate height steps in excess of 100 nm. As can be seen in Figure 1.8, after the first etch step the height difference will be many times larger. Planarization steps will, therefore, be required after each etch step, similar to what is done in CMOS processing. Also the requirements on wafer flatness are tighter than those that InP substrate manufacturers can provide today. Moving from I-line to 193 nm DUV lithography requires, therefore, major adaptations of the pro-

cess technology. Such process adaptations are presently being investigated by the JePPIX Technology Center, with support of ASML.

1.2.3 Planarization and Passivation

After the etching process the sidewalls of deeply etched phase modulators and detectors have to be passivated and protected as shown in Figure 1.8c. In the COBRA process this is done by deposition of a polyimide layer which also reduces the height difference on the chip (planarization). The passivation layer is necessary for obtaining low dark currents in reverse biased phase modulator and detector sections. Planarization is necessary in order to facilitate subsequent lithography steps, where the large difference in height between the different mesas complicates process steps like opening of the contact regions and definition of metal contacts. The planarization layer is also used as a substrate layer for metal interconnect between electrodes and bond or probe pads. It has a well-defined height at all mesas where contacts openings have to be made and it covers the mesas where metal crossings are required for interconnect purposes.

As explained in the previous section introduction of DUV lithography imposes much more stringent requirements on the surface planarity. Chemical-Mechanical Polishing can be used to meet those requirements.

1.2.4 Metallisation and Interconnect

The last process module is for contacting and metallisation as shown in Figure 1.8d. First the polyimide planarization layer is patterned lithographically and the remainder is etched back until the active mesas are opened. Next a thin Ti-Pt-Au contact layer is deposited with lift-off lithography for getting contacts with low series resistance. The alignment is not critical because the contacts are chosen wider than the mesa. After lift-off of the front contact the backside contact is deposited. Both contacts are annealed at the same time. For definition of bond pads and metal interconnect patterns the upper side of the wafer is covered with a thin gold seed layer, followed by a thick resist layer, which is opened where we need the metal paths. Next a thick gold pattern is electroplated through the openings in the resist mask and finally the whole gold pattern is etched back a little bit in order to remove the seed layer.

1.3 Building Blocks

1.3.1 Introduction

The basic idea behind a generic integration technology is to support the monolithic integration of a small set of accurately characterized building blocks that offer the basic functionality which is required to realize PICs for a broad range of different applications. Although the basic idea looks simple, its practical elaboration is not so straightforward, because the number of building blocks tends to become large: different types of lasers (FP, DFB, DBR, CW, pulse, tunable etc.), modulators, detectors, MMI-couplers (1×2 , 2×2 , 1×4 , 2×4 , 4×4 etc.) and AWGs with varying numbers of channels and channel spacings, to mention just a few. To utilize the full potential of the generic integration technology these building blocks have to be accurately characterized so that users can accurately design complex circuits based on them. A user designing a circuit based on these standard components will quite rightly ask for a guarantee from the

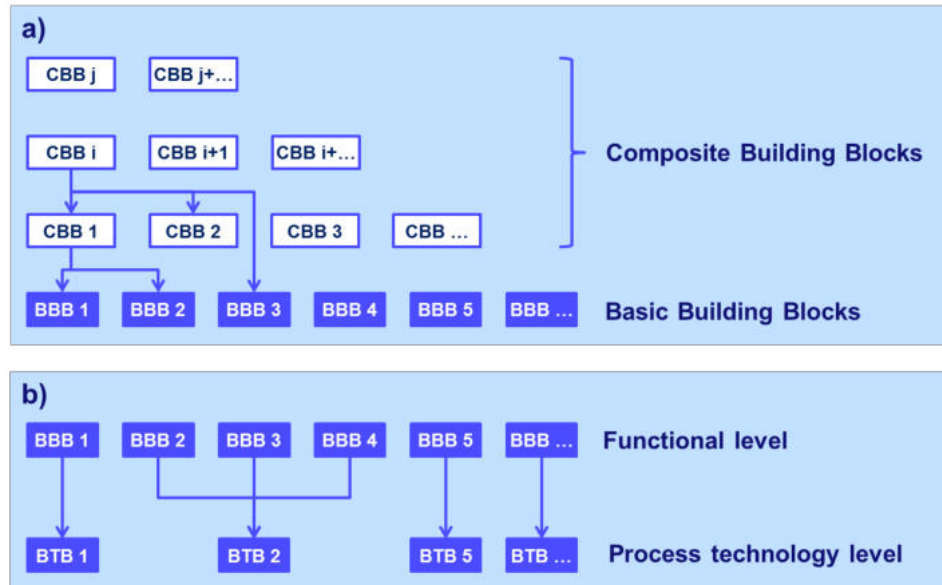


Figure 1.9: Schematic diagram of the hierarchical structure for the different building blocks. a) The Basic Building Blocks offer the basic functions available on the platform. A number of BBBs can be combined in Composite Building Blocks that perform more complex functions. They may also contain other CBBs. CBBs can have different levels of complexity, varying from a few up to a few hundred BBBs. b) The Basic Building Blocks form the lowest functional level of the platform. At a process technology level a number of BBBs with different functions may be realized from a single structure, which we call a Basic Technology Block.

foundry that the building blocks perform according to an agreed specification. Validating the proper performance of fabricated wafers will place a huge burden on the fab if approached in the wrong way, because the whole set of building blocks should be guaranteed for each MPW. Further, with so many different building blocks it will become a complex task to optimize the integration process: which building blocks should get priority in the process development?

In order to make the generic process development and validation manageable we distinguish between Basic Building Blocks (BBBs) and Composite Building Blocks (CBBs). The idea is to identify a small number of BBBs, which can be used to construct a much larger variety of Composite Building Blocks. In this way we create a hierarchy of building blocks in which the properties of the higher layers can be derived from the properties of the lowest layer, the BBBs. The scheme is depicted in Figure 1.9; it will be explained in some detail in the following chapters.

With this subdivision the optimisation and the validation of the generic process can now be focused on a small set of building blocks: the Basic Building Blocks. If their performance is optimized and validated, the performance of all PICs that are built from them according to the design rules should also meet the expectations. So instead of optimizing and validating a process for a huge number of different components, the foundry can focus all its efforts on optimizing and validating a small set of BBBs, which significantly reduces the technology development and validation burden.

	Basic Building Blocks	Abbr	2012			2015		
			Oclaro	HHI	COBRA	Oclaro	HHI	COBRA
1	Passive Waveguide	WG	●	●	●	●	●	●
2	Semiconductor Optical Amplifier	SOA	●	●	●	●	●	●
3	Photo Detector	PD	10 GHz	40 GHz	10 GHz	40 GHz	40 GHz	40 GHz
4	Saturable Absorber	SA	●		●	●	●	●
5	Electro-Refractive phase Modulator	ERM	10 GHz		10 GHz	40 GHz		40 GHz
6	Injection-type ERM	ERMI	1 GHz		1 GHz	1 GHz		1 GHz
7	Thermo Optic phase Modulator	TOM	●	●	●	●	●	●
8	Electro-Absorption Modulator	EAM					25 GHz	
9	Tunable Bragg Reflector	TBR	●			●		●
10	Electrical Isolation section	EI	●		●	●	●	●
11	Polarisation Rotation section	PR					●	●
12	Spot-Size Converter	SSC	●	●		●	●	●
13	Waveguide Termination	WGT	●	●	●	●	●	●

Table 1.2: Overview of the Basic Building Blocks available in the three foundry platforms, at present and planned for 2015.

1.3.2 Basic Building Blocks (BBB)

Basic Building Blocks (BBBs) are the smallest (irreducible) set of functional building blocks that are required to realize the full functionality provided by the generic technology. If a building block can be decomposed in more elementary building blocks then it is not a Basic Building Block but a Composite Building Block (CBB). A laser, for example, is composed of a gain section and a resonator, so it is a CBB. The resonator itself can be formed by a ring cavity, a Fabry-Perot (FP) cavity (two mirrors) or a Bragg grating. For an FP-laser, for example, the BBBs are a SOA section to provide the gain, and cleaved facets to form the cavity. The Semiconductor Optical Amplifier and the cleaved facets are BBBs since they cannot be decomposed into more elementary building blocks. A ring resonator is composed of curved and/or straight waveguide sections, so it is a CBB. The straight and curved waveguide sections themselves are BBBs. The arrows in Figure 1.9a illustrate how a CBB can be composed of a number of BBBs and/or CBBs.

Below a short description is given of the most important Basic Building Blocks available in the present generic integration processes at the JePPIX foundries. Although the different processes have a lot of BBBs in common, their performance may differ, and some building blocks are not offered by all foundries. Further, some building block epi-structures can be exploited to provide several different functions, a point which is expanded upon in section D below. Table 1.2 gives an overview of the different BBBs.

1. **Passive Waveguide section (WG).** Transparent waveguide sections are the most elementary building block in any generic process. They are used for interconnects and in Composite Building Blocks such as MMI-couplers and AWGs. They can be provided with different optical confinements, e.g. deep or shallow etched for strong or weak confinement. Their most important property is the propagation loss, which should be as low as possible.
2. **Semiconductor Optical Amplifier (SOA).** An SOA is an active waveguide section which provides gain to the guided signal when an injection current is applied.

Furthermore the non-linear operation of this BBB is interesting for many applications, e.g. in all-optical switching.

3. **Saturable Absorber (SA).** This is a reverse biased pin-doped absorbing waveguide section, which becomes transparent if sufficient e-h pairs are generated by the absorbed light to get population inversion (bleaching). A short reverse biased SOA-section can be used as an SA.
4. **Waveguide Photo Detector (PD).** A waveguide PD is an absorbing waveguide section provided with electrodes to carry the photocurrent. Its structure closely resembles that of an SOA and a short reverse biased SOA section can be used as a detector.
5. **Electro-Refractive Modulator (ERM, ERMI).** This is a pin-doped waveguide section in which a reverse (ERM) or a forward bias voltage (ERMI, current injection) induces a phase shift. The physical effects under reverse biased operation are very fast. With proper electrode design modulation as fast as 40Gb/s is possible. With current injection the speed is restricted to a few Gb/s by the carrier recombination time, and heating effects may degrade its performance.
6. **Electro-Absorption Modulator (EAM).** Electro-Absorption modulators are amplitude modulators. They operate at the band edge and use its bias-voltage dependence to modulate the absorption. They require a special pin-doped waveguide stack with a different epitaxial structure.
7. **Thermo-Optic Modulator (TOM).** A Thermo-Optic Modulator is a passive transparent waveguide section for which the phase transfer can be changed by heating it with a heater electrode on top of the waveguide. Modulation speeds are in the millisecond range.
8. **Tunable Bragg Reflector (TBR).** This is a pin-doped waveguide section with a periodic corrugation for which the peak reflection wavelength can be tuned by changing the bias current. It is a key device in tunable DBR or DFB lasers.
9. **Electrical Isolation Section (EI).** This is a waveguide section in which the highly p-doped top cladding has been removed or made highly resistive by proton implantation. It is used, for example, for isolating a forward biased SOA section followed by a reverse biased phase modulator from each other. Without such a section electrical crosstalk will reduce circuit performance.
10. **Polarization Rotation section (PR).** This is an asymmetric waveguide section (e.g. with an angled waveguide side wall) that has rotated modes and a strong birefringence. It can provide polarization rotation when properly connected to normal waveguides.
11. **Spot-Size Converter (SSC).** This is a BBB that adapts the size of the mode in the output waveguides of the PIC to better match the mode of a cleaved or lensed optical fibre or a dielectric interposer chip. In the current platforms these BBBs all use smoothly varying tapered waveguide cross-sections to achieve this function.
12. **Waveguide termination (WGT).** This is a device which is used for coupling light out of the PIC or for providing a low or high-reflection termination. It can be a simple cleaved facet or an etched facet, straight or angled (the latter for reducing reflection), and it may contain a high-reflection or anti-reflection coating.

1.3.3 Composite Building Blocks (CBB)

Composite Building Blocks are building blocks that are composed by combining two or more Basic Building Blocks and that do not require additional process steps for the combination. CBBs can be assembled by the designer using the design tools without reference to the process. For some of them the name CBB is counterintuitive: most designers will consider a junction between two different waveguides, an MMI-coupler or a Fabry-Perot laser not as a composite building block. As explained in the previous sections, in order to simplify the technology development and the process validation it is important to keep the number of Basic Building Blocks as small as possible, and this can only be achieved if we label all components that can be formed from BBBs without further adaption of the technology as CBBs. So a laser and an MMI coupler, but also a waveguide junction, are definitely composite building blocks. But also much more complex sub-circuits can serve as CBBs. Actually every sub-circuit that can be re-used as a building block in other ASPICS is a CBB. To enable its re-use it is important that it is made available to other users by including it in a component library that is provided to designers in the generic process: building an extensive CBB-library is an important target for generic platform technology development.

Where the distinction between BBBs and CBBs is not relevant we will call them just building blocks. Examples of CBBs are:

1. Junctions between a variety of waveguides:
 - Straight and curved waveguides
 - Waveguides with different (or opposite) curvature as used in S-bends
 - Waveguides with different widths (tapers)
 - Shallow and deep waveguides
 - Active and passive waveguides
2. MMI couplers, filters and reflectors:
 - Power splitters and combiners. Special case: 3-dB couplers.
 - MMI mode filters
 - TE-TM splitters and combiners
 - MMI-reflectors. These are MMI-couplers with a deep etched corner mirror at the end. They can be used as broadband on-chip reflectors.
3. AWG (de)multiplexers. Here a large variety in device specifications is possible: multiple input and output ports, different channel spacing, Free Spectral Range, channel passband width and shape (parabolic or flattened).
4. Lasers, such as Fabry-Perot lasers, tunable DFB and DBR lasers and (Mode-Locked) pulse lasers.
5. Mach-Zehnder or Michelson Interferometer modulators and switches
6. Switching matrices
7. WDM transmitters
8. Advanced receiver circuits, such as DQPSK or PM-DQPSK receivers

9. Actually any ASPIC can be used as a CBB in a more complex ASPIC.

BBBs and CBBs are made accessible for the designers by including them in a component library. The BBB library modules are provided by the foundries. The CBB library is expected to grow continuously, with a public and a designer-owned part. Designers can add their CBBs as modules to the component library and distribute them via the Process Design Kit on conditions that can be agreed between the owner of the module and the distributor of the Design Kit. In this way the library can be expanded with contributions from many designers. The potential of a generic integration technology is to a large extent dependent on the size and coverage of its CBB library.

1.3.4 Basic Technology Blocks (BTB)

Basic Technology Blocks are physical structures that can have different functions and that, consequently, can be used in different BBBs. An example is a Semiconductor Optical Amplifier: a short reverse biased SOA section can also be used as a detector. In table 1.2, the building block structures that can serve to create a number of different functions have been labelled in ***bold italics*** and the BBBs that can be derived from them in normal italics. It is seen that by realizing one or more Basic Building Blocks from a single Basic Technology Block the number of different technology blocks that the fabs have to integrate is reduced, which also reduces the complexity of the integration technology required. However, we will need to characterise their performance individually and provide different validation criteria. We will discuss two such basic technology blocks below.

Semiconductor Optical Amplifiers, if operated in reverse bias, can be used as detectors. If the active layer is bulk material, the detector performance can be quite good (bandwidth > 25 GHz). If the active layer is based on QW or QD-material the optical confinement and hence the absorption is lower and the detector length needs to be longer, which reduces the bandwidth and increases the dark current. The same structure can also be used as a Saturable Absorber in a Mode-Locked Laser. By using advanced epitaxial technology that provides design freedom in the choice of the band gap of the active layer stack (SAG technology) the number of BBBs in a generic process can be even further reduced: Electro-Absorption Modulators and detectors can then be realized in the same process as the SOAs.

Electro-Refractive Phase Modulators can be used both with reverse bias (depletion mode) and forward bias (current injection mode). Properties (electro-optic efficiency and bandwidth) will be significantly different. Further, if the electrode design is sufficiently flexible for use as a heater, they can also be used as Thermo-Optic Modulators.

If the lithography has sufficient resolution to support first order gratings (required resolution in the order of 100 nm) the phase modulators can also be used as tunable gratings, for example in DBR lasers. Usually these gratings are realized with E-beam or holographic lithography and epitaxial overgrowth techniques. If they can be realized with side-wall gratings in the same step as the waveguides, e.g. with DUV-lithography, we no longer need different technology steps for the phase modulators and the tunable gratings: they can be derived from the same modulator section used as basic technology block.

The basic technology blocks lead to very useful simplification of the process technology by using a single structure for a number of different functions. Whether such combinations are possible or not depends on the specific platform technology. Because the basic technology blocks support different functions and do not form a complete set, as

illustrated in Figure 1.9b, the basic functionality cannot be formed by the BTBs but only at the level of the BBBs, as indicated in Figure 1.9b. For the designers, the functional BBB-level is the starting point for the design, and the way in which the BBBs are formed in the integration process is not relevant for them.

1.4 Basic Building Blocks

In the following paragraphs we will discuss a number of Basic Building Blocks in some detail. Examples are taken from the COBRA process, because this was the first generic process that offered MPW services and most of the process and building block information is already in the public domain. In 2014 JePPIX has launched semi-commercial access to MPW-runs on platform processes of Oclaro, the Fraunhofer HHI and SMART Photonics. Semi-commercial means that the processes are not yet fully qualified (often referred to as 'beta release' for commercial devices). Numbers and features mentioned in the present text are representative of the building blocks offered by the JePPIX foundries, but because of steady development of these platforms, some specifications will differ from the actual values offered by the present platforms. For more actual and extensive information about the process specifications the reader is referred to the Design Manuals and the process specifications, which are available via the JePPIX platform [46] under NDA. Oclaro decided to stop open-access foundry service in 2016, HHI and SMART Photonics continued.

1.4.1 Passive Waveguide Sections (WG) and Electrical Isolation Sections (EI)

Transparent waveguide sections (WG) are the most elementary building block in almost any component. They are used for interconnection purposes and in composite building blocks like MMI-couplers and AWGs. They can be available with different optical confinements, e.g. deep etched (strongly guiding) or shallow etched (weakly guiding). Figure 1.10 (left, middle) shows an example of the cross sections of a deep and a shallow waveguide. The waveguide layer is a $0.5\ \mu\text{m}$ thick layer of Q1.25 bulk material. Q1.25 means quaternary material (InGaAsP) with a composition such that the band edge is at a wavelength of $1.25\ \mu\text{m}$ and the lattice constant is matched to the InP substrate. For shallow etched waveguides the ridge is etched $100\ \text{nm}$ into the waveguide layer. Deep etched waveguides are etched down to $> 150\ \text{nm}$ below the waveguide layer. Waveguide widths can be chosen by the designer, frequently used widths are $2\ \mu\text{m}$ for shallow waveguides and $1.5\ \mu\text{m}$ for deep etched waveguides.

Bend radii of deep etched waveguides can be as small as $10\ \mu\text{m}$. The advised minimum bend radius of shallow etched waveguides is in the order of $500\ \mu\text{m}$. Below $50\ \mu\text{m}$, significant polarization conversion can occur at the junctions between straight and curved waveguide sections if the side walls are not perfectly vertical. Waveguides with no significant polarization conversion were reported for radii down to $20\ \mu\text{m}$ [52].

Weakly guiding waveguides usually have the lowest propagation loss and are good for interconnection, but they do not allow for small-radius waveguide bends. Strongly guiding waveguides are preferred for compact components and small bending radii, but their propagation loss is usually higher. The propagation loss is caused by absorption losses due to free carrier absorption in the upper p-doped cladding layer and by scattering losses due to side-wall roughness of the waveguides. The cladding layers and the lower part of the waveguide layer are doped if the same waveguide structure

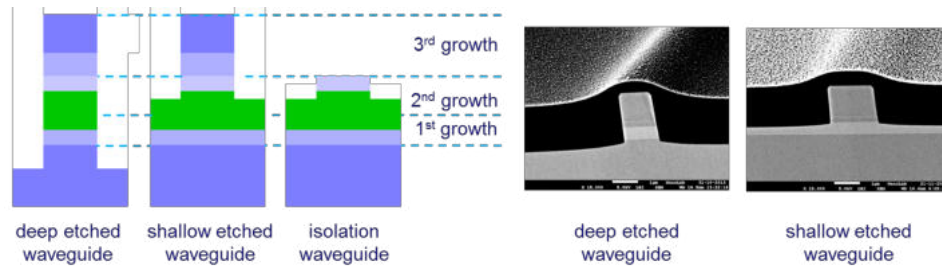


Figure 1.10: Left: Cross section of 3 passive Basic Building Blocks: a shallow etched waveguide (WGW), a deep etched waveguide (PWS) and an isolation waveguide section (EI). Right: SEM photographs of a deep and a shallow etched waveguide covered with polyimide (the apparent side wall angle is due to the perspective of the SEM photograph).

is used in the phase modulators. The n-type dopant has no significant contribution to the losses, but the p-dopant has. The upper cladding has a stepwise graded doping profile; it is lowest close to the waveguide where it interacts most strongly with the guided mode. Its minimum level is determined by the electro-optic efficiency of the phase modulator, which requires the pn-junction to be close to the waveguide. Good e-o efficiency can be obtained with a doping level that brings a propagation loss about 2 dB/cm. Lower losses (below 1 dB/cm) are possible with a more advanced integration process that avoids doping in the transparent waveguides.

Effective refractive indices of the shallow waveguides are in the order of 3.25 at 1550 nm wavelength. The birefringence of the shallow waveguides (effective index difference between TE- and TM-polarized modes) is in the order of $6 \cdot 10^{-3}$, which will cause a shift in the order of 3 nm (400 GHz) in wavelength sensitive devices like AWGs and DBR gratings. For deep etched waveguides it crosses zero at a waveguide width of 1.5 μm , but it is very sensitive to small width deviations. A width deviation of 50 nm already causes a (wavelength dependent) birefringence variation of a few times 10^{-4} , corresponding to a TE-TM shift up to 100 GHz in an AWG.

Electrical Isolation Sections (EI). The high dopant level of the upper cladding provides a resistive path between all active components connected by a waveguide, such as SOAs, detectors and modulators. If these components operate at different voltages (e.g. forward and reverse bias) large leakage currents can occur which may change the operating voltages over the components (cross-talk). To prevent such a leakage current an electrical isolation waveguide section (EI), as shown in Figure 1.10, has to be inserted between the two components. The resistance of this section, which is strongly increased by removing the highly doped upper cladding, is in the order of 20 k Ω per μm section length. The isolation section has slightly increased propagation loss, so it should not be made longer than necessary. The transition between a waveguide and an isolation section also introduces small additional loss. Possible reflections at this interface are reduced using an angled isolation etch.

A more detailed description of the waveguide building block is given in chapter 9. The underlying physics is described in chapter 2.

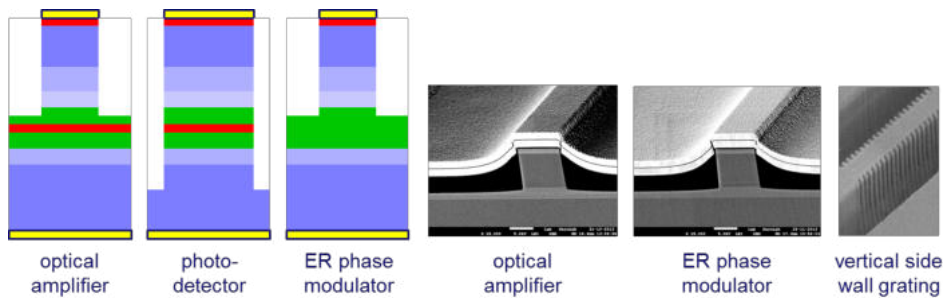


Figure 1.11: Left: Cross section of a semiconductor optical amplifier (SOA), a waveguide photo detector (PD) and a phase modulator (ERM). Right: SEM photographs of a SOA, a phase modulator and a vertical side wall grating (the apparent side wall angle is due to the perspective of the SEM photograph).

1.4.2 Optical amplifiers (SOA), Photo Detectors (PD) and Saturable Absorbers (SA)

Semiconductor Optical Amplifiers (SOA) provide gain to an optical input signal, they are, therefore, also called gain blocks. An important feature of the butt-joint epitaxial regrowth process is the modular character of the gain block: the integration process is not sensitive to the composition of the gain blocks, as long as the total thickness of the active waveguide layer is not changed. The process can be used, therefore, for bulk active layers (120 nm Q1.55 material) as well as for Quantum Well (QW) or Quantum Dot (QD) active layers with different emission wavelengths. The active layers are embedded in a Q1.25 separate confinement layer, and the total thickness of the active waveguide stack is 500 nm. All layers have their gain maximum around 1550 nm at appropriate current injection levels.

For the MPWs an MQW layer stack embedded in a 500 nm Q1.25 layer is used. The standard SOA ridge width is 2 μm . The SOA is shallow etched in the same etching step as the shallow waveguides. A shallow etch is applied in order to avoid the etch reaching into the active layer, which causes increased surface recombination. Figure 1.11 (left) shows the cross section. An 800 μm long SOA section has a gain of 20 dB at an injection current of 120 mA.

For detection purposes a reverse biased deep etched SOA with 10 μm width is used as a photodetector (PD), as shown in Figure 1.11 (middle). It allows designers to connect any shallow or deep waveguide of equal or smaller width directly to the detector. The increased width also increases the input power levels at which saturation occurs. Dark currents are lower than 1 nA/ μm detector length. With a bulk active layer a section length of 50 μm is sufficient to absorb more than 95% of the incident light, with a QW active layer the detector becomes significantly longer. For bulk active layers the detector capacitance and transit time are sufficiently small to allow operation speeds well beyond 10 Gb/s, with QW active layers a special design with slightly lower responsivity is required for 10 Gb/s operation.

The HHI-platform offers excellent high-speed detectors with > 35 GHz bandwidth, 0.8-0.9 A/W responsivity and dark current < 5 nA (@ -3 V). Because the platform uses SI substrates the detectors can be used in balanced configuration.

A short section with a reverse biased SOA structure can also be used as a saturable absorber (SA) for use in Mode-Locked lasers.

An important improvement of the capabilities of the platforms can be obtained by in-

roducing Selective Area Growth (SAG) technology which offers designers a free choice of the bandgap of active components, as described in Section 1.2.1.

A more detailed description of the design of optical amplifiers, detectors and saturable absorbers is given in chapters 14, 15 and 16, respectively. The underlying physics is described in chapter 3.

1.4.3 Modulators (ERM, ERMI, TOM, EAM)

Figure 1.11 (left schematic) shows the cross section of a phase modulator (Electro-Refractive Modulator, ERM), which is fabricated in the same waveguide stack as the passive waveguides. It can be realized both with a shallow or deep etched waveguide and its design is a trade-off between phase modulation efficiency in the modulator section and propagation loss in the transparent waveguide. The modulator has a pin-structure in which the phase modulation is caused by a number of effects. The most important effect in a bulk-type modulator section is carrier depletion in the waveguide layer when a reverse bias voltage is applied. In a QW-type modulator section the dominant effect is the Quantum-Confined Stark effect which causes an effective index change when the voltage over the QW-stack is changed. The phase modulation efficiency is usually characterised by the $V_{\pi}L_{\pi}$ - product. Bulk-type modulators can have $V_{\pi}L_{\pi}$ - products in the order of 10 Vmm, i.e. with an electrode length of 2 mm a phase shift of 180° is obtained with 5 V. QW-modulators can have efficiencies that are 3-4 times larger, so that the $V_{\pi}L_{\pi}$ - product is 3-4 times smaller. Short modulators can operate at frequencies well beyond 10 GHz, with special electrode design bandwidths of 30-40 GHz are possible.

The modulator section can also be used with forward bias (current injection, ERMI), phase modulation efficiency can be $>100^{\circ}/\text{mA}$ for a 1 mm long modulator section. The bandwidth for phase modulation is small, it is restricted by the carrier recombination time (ns) and it can be further reduced by slow heating effects.

Heating is a simple way to change the phase transfer of a waveguide, the refractive index of InP changes with $6 \cdot 10^{-5}/\text{K}$. This means that for a 500- μm -long waveguide (which has an optical length of about 1000 wavelengths) a temperature change of 50 K causes a phase change of about 180° . Modulation efficiency in a 500- μm -long modulator section is typically in the order of 180° for 25 mW heating power. Thermo-Optic (TO) Phase Modulators can be realized in the same process as the electro-optic modulators, by feeding a current through the electrodes and using their resistance to generate heat. TO modulators show a much weaker wavelength dependence than electro-refractive ones. Modulation speed is in the millisecond range.

In static or quasi-static applications phase modulators are often denoted as phase shifters. Technically speaking, there is no difference, except for the bandwidth, which can be low if the electrodes are not designed for rf-operation. In this article we will use the term modulator for both high-speed modulators and low-speed phase shifters.

Electro-Absorption Modulators (EAM) have a similar (pin-doped) structure as MQW Electro-Refractive Modulators. The main difference is in the bandgap wavelength of the modulator section, which should be close to the signal wavelength. The bandgap of an EAM can be shifted by applying an electric field across the MQW section (by the Quantum-Confined Stark Effect). Because the EAM is operated close to the band edge, it has a significant absorption, which can be changed by applying a voltage. In this way the amplitude of the transmitted signal can be modulated. EAMs can operate with low voltages and shorter lengths than ERMs, dependent on the required Extinction Ratio. They have been reported with bandwidths up to 50 GHz. A disadvantage of EAMs is

their higher insertion loss, typically several dBs, and their dispersive properties: they introduce a frequency chirp to the modulated signal.

A more detailed description of the design of electro-refractive, thermo-optical and electro-absorption modulators is given in chapters 17. The underlying physics is described in chapter 3.

1.4.4 Tunable Bragg Reflector Gratings (TBR)

Tunable waveguide gratings can be used to form tunable DBR-lasers by placing them on one or both sides of a SOA gain section. They are usually formed by a periodic corrugation of the lower or upper waveguide surface, using epitaxial overgrowth after etching of the grating structure. The peak reflection wavelength can be tuned by current injection in the pin-doped waveguide. The designer can choose the peak wavelength and the reflection coefficient through the periodicity and length of the grating. In general, the coupling strength of the grating cannot be varied over the wafer; it is fixed for a certain MPW-run, even though it could be changed between different runs.

If the grating can also be applied in a SOA section, it supports the design of DFB lasers. In principle, the gratings can also be etched in the side walls of the waveguides, as shown in Figure 1.11 (right), using DUV lithography. Side-wall gratings allow control to be released to the designer so that the grating period, length and coupling strength may be freely chosen, and the gratings can be realized together with the modulators without additional process steps.

A more detailed description of the design of waveguide gratings is given in chapters 12.

1.4.5 Polarization Rotation Sections (PR)

With the BBBs discussed above we can manipulate the amplitude and phase of the optical signal. A third important property of the light is its polarization. For polarization manipulation and control we need another basic building block: a polarization rotation section (PR). The PR consists of a deep etched waveguide with a straight and an angled sidewall, in which the two polarization modes are rotated by 45° and have a difference $\Delta\beta_{\text{pol}}$ in propagation constant. If both modes are excited with the same amplitude at the junction with the straight waveguide they will start beating, and after a length $L = \pi/\Delta\beta_{\text{pol}}$ one polarisation component will have opposite sign and the polarisation will be rotated by 90° . When integrated between two normal waveguides it acts as a half-wave plate, which rotates the incoming polarization (either TE or TM) by 90° . So the combination of a polarisation rotation section and two waveguide junctions acts as a Polarisation Converter (PC). The length of a 90° PR section is typically in the order of $100\ \mu\text{m}$. A polarization splitter or combiner can be realised by integrating two PCs in the arms of an MZI, as depicted in Figure 1.12 [53]. By integrating phase shifters between a polarization splitter and a combiner we can obtain full control over the polarization state. The PC illustrates how we can add all the functions required for on-chip polarization manipulation (polarization conversion, polarization splitting and combining, and dynamic polarization control) by adding only one BBB, a PR, to the generic integration scheme.

The tolerance requirements for a single-section PR are very tight, the width has to be controlled within 50 nm. COBRA has developed an improved double-section PC with better process tolerance [54], which makes integration in the present technology platforms feasible. With advanced DUV lithography Critical Dimension (CD) control will be sufficient for supporting both the improved and the original versions of the PC.

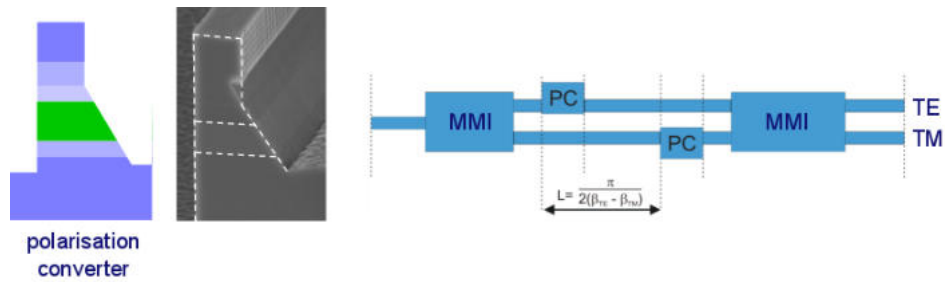


Figure 1.12: Schematic cross section (left) and SEM-photograph (middle) of a polarization rotation waveguide section. Right: Circuit scheme of a polarization splitter based on a Mach-Zehnder Interferometer with two polarization converters.

A more detailed description of the design of polarisation rotation sections is given in chapter 11.

1.4.6 Spot-Size Converters (SSC)

Fibre-Mode Adapters or Spot-Size Converters (SSC) are crucial building blocks for efficient and tolerant coupling of light from the chip to one or more fibres. The converter acts as an optical funnel, adapting the small mode diameter of the waveguides on the chip to the mode size of a cleaved or lensed fibre. For a high coupling efficiency and good fabrication tolerance, the converter expands the horizontal and vertical diameter of the mode adiabatically [55, 56]. A vertically tapered waveguide section, as depicted schematically in Figure 1.13, forces the light from the high index passive waveguide section on top, to a low contrast Fibre-Matched Waveguide (FMW) formed below the high index waveguide. The FMW carries a larger mode which allows for efficient and tolerant coupling to a cleaved or lensed fibre or a dielectric interposer. The FMW can be formed either by a thick n^- -doped InP layer, which has a higher refractive index than the high doped (n^+) substrate, or as a so-called diluted waveguide, which has a few (typically three) thin quaternary layers between thicker InP barrier layers.

Good SSCs have 0.5-1 dB coupling loss to a lensed or cleaved fibre or an interposer chip with $3\ \mu\text{m}$ spot diameter and they can have a small pitch ($25\ \mu\text{m}$), which makes them suitable for integration in dense arrays [57].

Concentrating the SSCs in dense arrays, e.g. for switching matrices, is useful for reducing the chip area occupied by the SSCs. For such dense arrays an interposer chip of dielectric waveguide material is required to couple the signals out of the chip, as fibre diameters are typically $125\ \mu\text{m}$ and the pitch is 127 or $250\ \mu\text{m}$. The interposer can be used to adapt the pitch of the SSC-array to that of a fibre array, but it may also contain passive devices like delay lines and high-Q filters with better performance than offered by the InP chip because of the lower losses of dielectric waveguide platforms (< 0.1 dB). In this way it may serve as a hybrid platform, combining the best of InP and dielectric waveguide technology, and the dense SSC array serves as an optical bus between the two chips. The JePPIX partners are cooperating to develop such a hybrid platform technology.

An SSC can also be fabricated using lateral tapering of the upper waveguide to push the mode down to the FMW. If the lateral taper is written in the same lithography step as the waveguides this leads to a reduction of the number of process steps. It requires a high resolution and dimensional control of the lithography, which is feasible with DUV

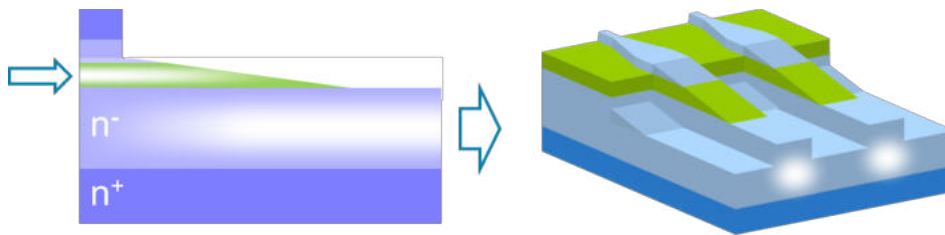


Figure 1.13: Left: Cross section of a vertically tapered Spot-Size Converter illustrating how the mode of the upper waveguide is coupled to a waveguide with a larger mode diameter. Right: 3D picture illustrating how the SSCs can be integrated in dense arrays.

lithography.

A more detailed description of the design of tapers and spotsizes converters is given in chapter 21.

1.5 Composite Building Blocks

A *composite building block (CBB)* is any combination of two or more basic building blocks (BBB). Whether we call such a combination a CBB or not depends on its potential for re-use: if it can be re-used as a building block in a more complex circuit it is a CBB. So MMI-couplers and AWGs are CBBs, but also more complex sub-circuits like a full DQPSK receiver can be a CBB if it is used as a building block in a more complex ASPIC. CBBs can be parameterized: in a WDM transmitter consisting of a set of DBR lasers and an AWG for multiplexing the WDM signals, the DBR laser is a CBB. But to avoid that we end up with a separate CBB for every wavelength we can enter the emission wavelength of the DBR laser (determined by the period of the DBR grating) as a parameter, so that we can build a full DBR laser array with a single CBB. And for an AWG, for example, we may enter the central wavelength, the channel spacing, the FSR and the bandpass shape as a parameter.

A CBB can be re-used by a designer in his own ASPIC. But it is much more useful if it is stored in a component library so that every designer who has a licence for that library, can use it. The most important modules to be stored in a CBB-library are a mask layout generation module and a simulation module which the designer can use in a circuit simulator. CBB libraries are usually part of the Process Design Kit (PDK) which is provided by the foundries or a broker to designers that want to participate in an MPW run. The application potential of a foundry process is, to a great extent, determined by the number and the quality of the CBB-modules that are available in the library. Building an extensive CBB-library is a major task and a continuing effort for developers and users of a foundry process, which will lead to a steady increase of the application potential of the process.

Below we will briefly describe the most frequently used Composite Building Blocks.

1.5.1 Junctions between Different Waveguides

Any ASPIC will have different types of waveguide, straight and curved, shallow and deep etched, active and passive, and waveguides with different widths. Each waveguide has its own mode-profile, and some of them can carry several modes. If we just

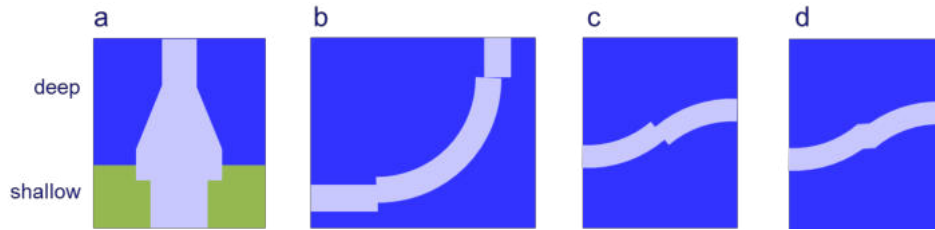


Figure 1.14: Junctions between different types of waveguides: a) shallow and deep etched waveguides; b) straight and curved waveguides; c) curved waveguides with opposite curvature; d) same as c) but with angled facets for low reflectivity.

connect them we will introduce coupling loss and back reflections at the junction. For maximal coupling and minimal back reflection the junctions have to be carefully designed.

The junctions described below do not incur additional process complexity, they can be realized by the designers using standard BBBs or, as in the case of deep to shallow waveguide matching elements, be offered by the platforms as CBBs using the same basic process sequence. They can have physical dimensions, but some of them consist just of an offset between two waveguides, which is optimized to reduce the junction losses. If properly designed, junction losses will be small (typically lower than 0.1 dB) and reflections low (< -40 dB). For accurate designs their properties, like transmission loss, back reflection and mode conversion (including coupling to radiation modes) should be accounted for in the circuit simulation. The most important junctions are the following:

- **Shallow-deep junctions**

Figure 1.14a shows a top view of a low-loss junction between shallow and deep waveguides. At the junction the deep etched waveguide is a bit wider than the shallow one in order to get an optimal match between the mode profiles in both waveguides. Further, the wider waveguide section is extended a few μm into the shallow region to avoid the possibility of a deep slit occurring between the deep and shallow etched waveguide due to a small mask misalignment. The junction is followed by a taper because the standard deep etched waveguides are narrower than the shallow etched ones. For minimal reflection the interfaces should be angled.

- **Straight-curved and curved-curved junctions**

Junctions between straight and curved waveguides are shown in Figure 1.14b. Here an offset and a width adjustment are applied to get an optimal match between the mode profiles in the straight and the curved waveguide, where the mode shifts to the outer edge and is slightly compressed. Junctions between curved waveguides with opposite curvature (Figure 1.14c) have an offset which is approximately twice the offset between a curved and a straight waveguide. The abrupt offsets as depicted in b) and c) may cause small reflections. These can be reduced by applying angled facets as shown in Figure 1.14d. They will have negligible effect on the transmission, but lead to a significant reduction of the back reflection. Another way of reducing back reflection is to apply a slow change of the curvature (approximating an adiabatic transition). This can also reduce the small amount of mode conversion that occurs at an abrupt junction, but at the cost of a significantly larger length of the total bend.

- **Active-Passive junctions**

Whereas the junctions between passive waveguides offer the designer some design freedom, the design of junctions between active and passive waveguide sections is usually fully determined by the process developer (the foundry). For accurate design their physical properties, such as coupling loss, back reflections, mode conversion and radiation have to be included in the modelling. Back reflections play an important role, especially in circuits with a high gain, where they will lead to fringes in the wavelength response, and at high gain values they may cause poor side mode suppression or even lasing at undesired wavelengths. For good junctions back reflections are below -40 dB. Even at this level they can have visible effects, however.

- **Tapers between waveguides with different widths**

In order to avoid mode mismatch loss and back reflections a taper is used to connect two waveguides with different width. The loss can be very low, if the taper angle is chosen sufficiently small (adiabatic tapering). Taper length increases quadratic with the width. For large taper ratios a parabolic tapering profile is, therefore, optimal. For small taper ratios a linear taper is adequate. A taper from a 2 to 3 μm wide shallow waveguide requires a length of about 50 μm , tapering from 2 to 1.5 μm requires about 20 μm .

1.5.2 MMI-components

1.5.2.1 MMI-couplers

Combining and splitting of signal power are basic functions in almost any circuit. It can be done with star couplers, directional couplers or MMI-couplers. Star couplers are good for high splitting ratios, but they have significant non-uniformity and splitting loss. Directional couplers can have very low insertion loss and back reflections, but in high-contrast waveguide technology the gap between the waveguides needs to be submicron and it is difficult to control the coupling ratio accurately. MMI-couplers [58, 59] are, therefore, the most frequently used couplers.

An MMI coupler is a multimode waveguide section in which single or multiple copies of the field at the input facet are imaged on the output facet. The imaging is based on decomposition of the input field into the modes of the MM-section and reconstruction of single or multiple images at certain lengths, where all the modes arrive with the proper phase. The imaging properties are dependent on the MMI-section length and the position and shape of the input and output waveguides. Figure 1.15 shows the schematic layout of MMI-couplers (a) used as 1×2 power splitters or combiners and (b) 2×2 couplers. They can be realised both in shallow and deep waveguide technology. The imaging quality, and hence the insertion loss and the crosstalk are better for a deep etched MMI-section, but the reflections at the end faces are lower for a shallow etched coupler. MMI-couplers with deep etched sidewalls and shallow etched end faces (as shown in Figure 15), combine both advantages. Further reduction of reflections can be achieved by applying angled facets [60] as indicated in Figure 1.15c or even more sophisticated shapes of the end facets [61]. They prevent that light reflected at the end facet can couple back to the input port.

1.5.2.2 MMI-filters.

MMI-couplers with one input and one output port, as depicted in Figure 1.15d, can be used as mode filters [62]. When properly designed they transmit the fundamental

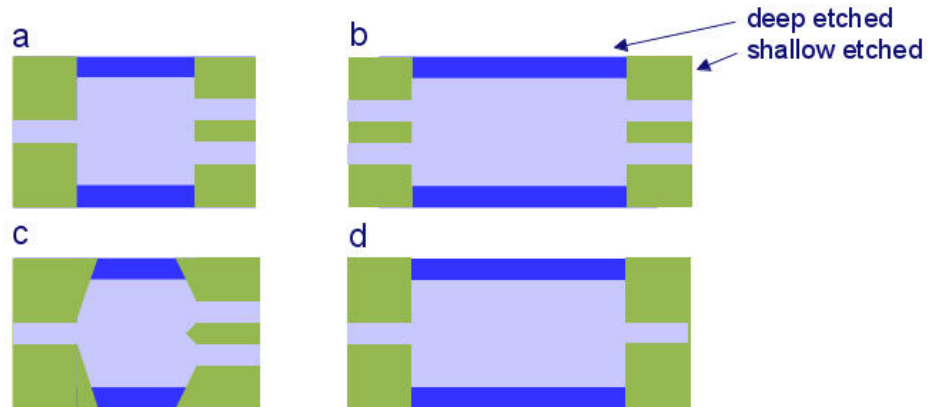


Figure 1.15: Multimode interference (MMI) couplers and filters: a) 1×2 power splitter or combiner b) 3-dB coupler c) MMI-coupler with angled facets for reducing end facet reflections d) first-order mode filter

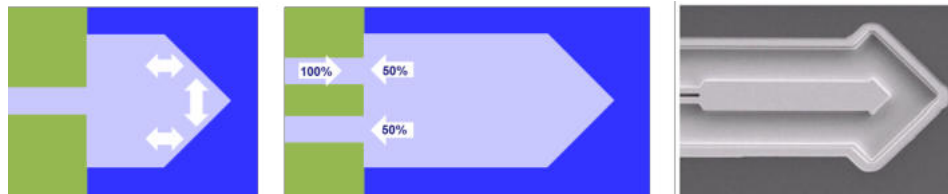


Figure 1.16: MMI-Reflector with total reflection (left) and partial reflection and transmission (middle). Right a SEM photograph of a MIR with a reflection and a transmission port, surrounded by a deep trench. The MIR shown in the photograph has no shallow input waveguides.

mode and suppress the first order mode, which can be excited at asymmetrical junctions in the waveguide or by reflection at angled facets.

1.5.2.3 MMI-reflectors.

On-chip reflectors are important components for flexible design of Fabry-Perot cavities (e.g. in lasers), because they can be placed everywhere on the chip. This avoids the need of positioning the cavity at a cleaved end face and it also allows better control of the dimensions of the cavity. Further, on-chip reflectors allow for on-wafer testing of devices, because the wafer need not be cleaved in order to obtain the laser mirrors. The most commonly used way to fabricate on-chip reflectors is by using DBR or DFB gratings. This requires high-resolution lithography, either DUV, holographic or E-beam. A simple way to realize a reflector in a shallow-deep etching process is by providing a 1×2 MMI coupler with a corner mirror at the end facet for obtaining total reflection, as depicted in Figure 1.16 (left). The corner mirror consists of two deep etched (totally reflecting) 45° mirror facets. The two images will be reflected by the two mirrors, which work as a corner reflector, and focused back on the input waveguide. The component can be considered as a folded 1×1 coupler with twice the length of the 1×2 coupler, in which the folding line is replaced by a corner mirror. In this way mirrors with less than 1 dB reflection loss can be realized. We call them Multimode Interference Reflectors, abbreviated MIRs. If two waveguides are connected at the input, the signal coupled

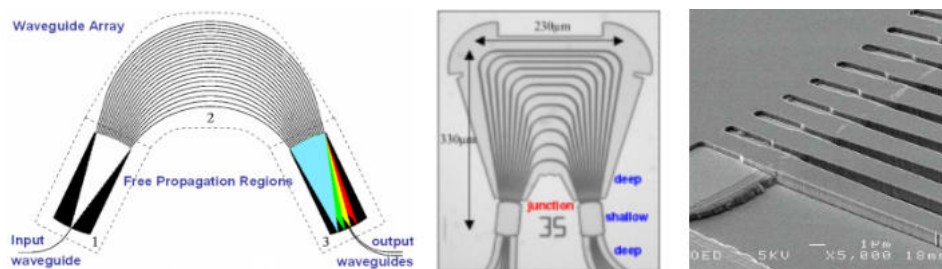


Figure 1.17: Left: Schematic picture of an AWG demultiplexer. Middle: Compact 4-channel AWG with combined shallow and deep etched waveguides. Right: SEM picture of the region around the junction between the waveguide array and the FPR, showing the closing of the gaps and the tapered shallow-deep waveguide junctions.

into one input is reflected back into both waveguides, as depicted in Figure 1.16 (middle), so that the component works as a partially transmitting mirror. By folding 2×2 couplers or asymmetric MMI-couplers 50/50 and 85/15 transmission and reflection ratios can be obtained, and with tapered MMI-couplers any desired ratio can be realized in principle [63]. A distinct feature of MIRs as compared with DBR or DFB-mirrors is their broad spectral width.

1.5.3 AWG (De)Multiplexers and Routers.

Arrayed Waveguide Gratings or PHASARs, as they were called in the early days, are widely applied as wavelength (de)multiplexers, routers and filters [64]. AWGs have been reported with both shallow and deep etched waveguides. Shallow etched AWGs can have losses below 2 dB, but they are rather large (several mm) because of the large bending radii in the waveguide array. Deep etched AWGs can be much smaller, but have larger losses (typically > 5 dB). The losses occur at the junction between the waveguide array and the Free Propagation Regions (FPR), as shown in Figure 1.17 (left). For low loss, the gaps between the array waveguides close to the FPR should be very sharp so that the guided modes in the array will couple adiabatically to the slab waves in the FPR and vice versa. Due to the characteristics of the etch process and the finite lithographic resolution the gaps will close abruptly, however, which causes a discontinuity that will introduce scattering and reflection losses. Because of the high contrast these losses can easily exceed a few dB per junction. A solution to that problem is the application of combined deep and shallow etched waveguides [65], as depicted in Figure 1.17 (middle). Both the array waveguides and the receiver and transmitter waveguides are deep etched, which leads to very small array dimensions: $330 \times 230 \mu\text{m}$ for the 4-channel device shown in the figure. The deep etched region can be seen in the figure as the complex shaped box around the AWG. Figure 1.17 (right) shows a SEM-picture of the junctions between the FPR and the waveguide array, and between the shallow and deep etched waveguides. The closing of the gaps is clearly seen. Because the discontinuity occurs in the shallow etched region it brings much lower loss and reflection. The tapered junctions from shallow to deep waveguides, as schematically depicted in Figure 1.14a, can also be seen in the SEM-picture. Using DUV lithography the closing of the gaps occurs at much smaller gap widths and using DUV-lithography, low-loss AWGs have been reported with deep etched waveguides only [66].

In AWG-design, a large variety of device specifications is possible: number of input and output ports, channel spacing, Free Spectral Range (FSR), bandpass shape (parabolic

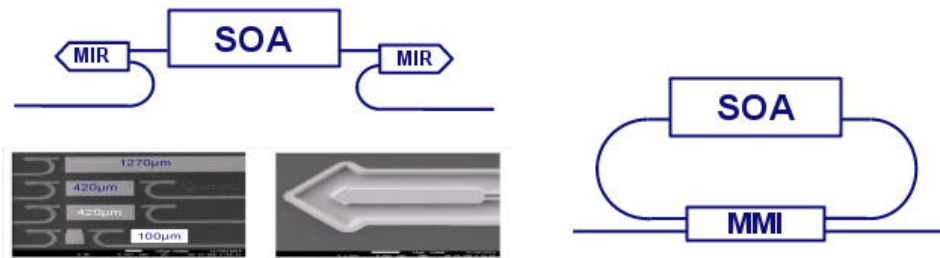


Figure 1.18: Left: Schematic and SEM photograph of a Fabry-Perot laser formed by a SOA section integrated between two broadband MIR reflectors. The waveguides are embedded in a deep etched trench. Right: Schematic of a ring laser.

or flattened), just to mention the most important ones. The most practical way to cover this variation an AWG design is by using a number of different library modules. By parameterizing the module so that it can handle designs with different channel spacings, FSRs and possibly also different numbers of input and output ports, the number of modules required for the most common operations may be reduced to a few. The current AWG libraries cover parameterized designs.

1.5.4 FP-lasers and Ring Lasers

The first semiconductor lasers were Fabry-Perot lasers. They were realized by fabricating an array of active SOA waveguides on a wafer, cleaving the wafer into bars, and cleaving the bars into individual laser chips. The cleaved facets were used as reflectors, without coatings they have a reflectivity in the order of 30%. The length of the cavity was determined by the cleaving of the bars. Fabry Perot lasers are typically multimode lasers, they will lase at a number of longitudinal cavity modes simultaneously. The modes are spaced by the so-called Free Spectral Range (FSR), which is determined by the length of the FP-cavity. Recently Fabry-Perot lasers were used as building block in single-mode lasers. In these lasers the FP-laser is forced to operate in a single FP-mode using filtered feedback [67]. The FSR is matched to the ITU wavelength grid, so that the cavity length needs to be controlled very accurately. This is not possible with cleaving. Figure 1.18 (left) show a schematic and a SEM-photograph of an FP laser which has been formed by using MIRs as broadband reflectors instead of the cleaved facets. In this way the cavity length can be controlled much more accurately. A way to form a laser without reflectors is by using a ring cavity, as shown in Figure 1.18 (right).

1.5.5 DBR and DFB-lasers

Another and more common way to make lasers single-mode is by using gratings as wavelength selective reflectors. If we replace the two MIRs in Figure 1.18 with gratings, we get a DBR laser. If we use tunable gratings we get a tunable DBR laser. Gratings can be tuned by current injection to give a change in effective refractive index in the region of -0.02 , sufficient to tune the laser over approximately 10 nm in the 1550nm wavelength band. By optimizing the reflectivity of the front and rear-gratings (choosing a proper grating length) and by including a phase shifter in the cavity, a tuning range of 5-8 nm can typically be realized, while maintaining single frequency operation with high side-mode suppression ratio (SMSR) [68]. For larger tuning ranges more sophisticated designs are required, e.g. [69].

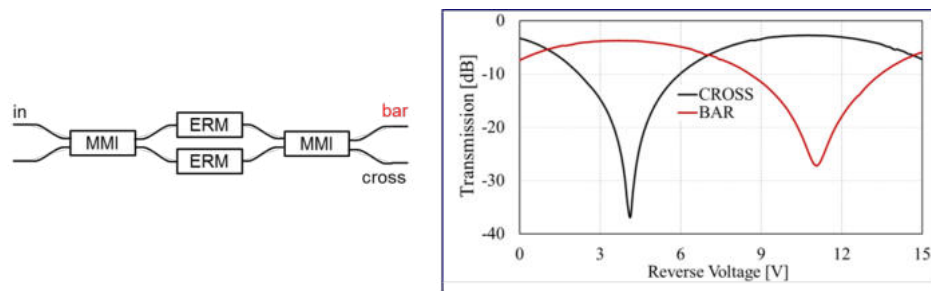


Figure 1.19: Left: Schematic of a Mach-Zehnder and (right) switching curve of a Mach-Zehnder with 2 mm long electrode.

In DFB lasers, as opposed to DBR lasers, the reflecting grating is incorporated into the gain section itself by placing it above or beneath the active region, or at the sidewalls.

1.5.6 MZI and MI-modulators

An amplitude modulator or a space switch can be obtained by putting one or two phase modulators in the branches of a Mach-Zehnder Interferometer Modulator, formed by two MMI-couplers. By applying 180° phase shift in one of the arms, the input signal can be switched from the cross port to the bar port. Figure 1.19 shows a schematic and a typical switching curve of a Mach-Zehnder interferometer modulator, which can also be used as a space switch. Switching voltages at 1550 nm are between 3 and 4 V for a 1 mm long electrode with MQW modulator sections, and around 7 V for a 2 mm long electrode using a bulk-type modulator. The switching voltage is both polarization and wavelength dependent. The electrode length and the capacitance can be reduced by a factor of two by using the phase modulators, combined with a reflecting element (cleaved facet or MMI reflector), in a Michelson Interferometer (MI) configuration.

The composite building blocks discussed above are only a few of the most important building blocks. Many other CBBs like DQPSK receivers, switching matrices and complex lasers can be fabricated on the generic platforms and will be investigated and included in the component libraries.

1.6 ASPIC Examples

In this chapter we give some examples of Applications Specific Photonic ICs (ASPICs) that have been realized in the generic foundry processes of COBRA and SMART Photonics, Oclaro⁵ and the Fraunhofer HHI. Most of the examples have been developed in the framework of the EuroPIC [41] and PARADIGM [42] projects, and some of them in two Dutch national projects: MEMPHIS [43] and the IOP Photonic Devices [44]. In chapter 27 we will elaborate a number of PIC designs in more detail.

1.6.1 COBRA & SMART Photonics Platform

COBRA has been pioneering with the development of generic integration processes since the beginning of the century [39]. Since 2007 it has provided access to its generic

⁵Oclaro has stopped offering foundry access in 2016

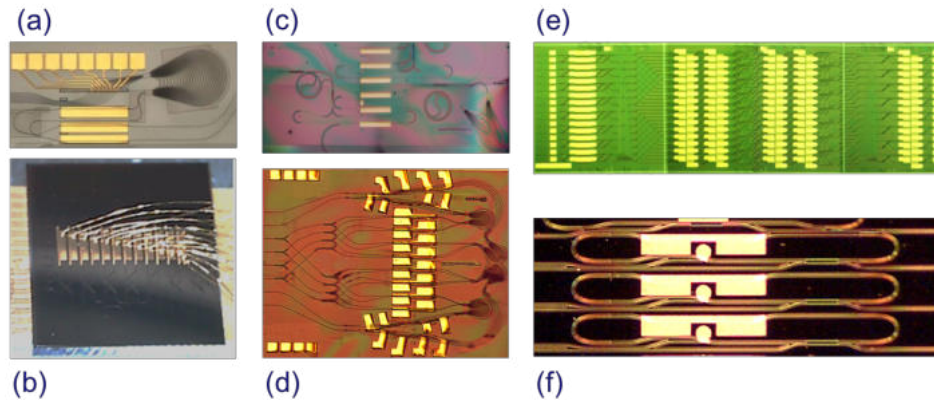


Figure 1.20: Examples of Photonic ICs realised on the generic COBRA platform. a) AWG-based discretely tunable laser with nanosecond switching speed ($1.5 \times 3.5 \text{ mm}^2$); b) 320 Gb/s Monolithic multistage SOA switching circuit, c) Multifunctional delay interferometer ($4 \times 2 \text{ mm}^2$); d) 4×4 Space and wavelength selective cross-connect ($4.2 \times 3.6 \text{ mm}^2$); e) Monolithic 16×16 photonic switch for broadband photonic packet-routing ($4.0 \times 13.2 \text{ mm}^2$); f) Broad frequency comb laser ($0.3 \times 2.2 \text{ mm}^2$).

integration process for research purposes to external partners, in the framework of the JePPIX platform [46]. In 2013 COBRA-spinoff SMART Photonics began offering (semi-) commercial access to this platform, while COBRA continued working on extensions to the capabilities of InP-based generic integration technology as described in the previous chapters. Below some examples are given of chips realised in the COBRA & SMART Photonics process.

Fast Discretely Tunable Laser Figure 1.20a shows an AWG-based discretely tunable laser with nanosecond switching speed based on a novel concept [70]. It uses a booster amplifier in the common waveguide of the AWG and short SOA gate switches in the waveguides connected to the demultiplexed side of the AWG. These short SOAs can be switched within a few ns with currents as low as 1 mA. Laser peaks have side mode suppression ratios of 30–40 dB. The switching between AWG channels is discrete and no laser operation takes place at wavelengths corresponding to other channels during the tuning process (dark tuning). This makes the device promising for packet routing and switching applications.

320 Gb/s Switching Matrix Figure 1.20b shows a multi-stage interconnection chip with nanosecond reconfigurability and a demonstrated capability of routing 320 Gbit/s line-rate signals [71, 72]. The chip comprises twelve pairs of SOA gate switch elements which are wire bonded to a ceramic carrier. Two pairs of SOA gates form a crossbar switch composite building block. Six such building blocks are then implemented to connect four input ports with four output ports in a four stage network. All of the input and output waveguides are accessed via the front facet of the chip and placed at a pitch of $250 \mu\text{m}$ for packaging compliance. This is the first active-passive multistage circuit reported.

Multi-functional Delay Interferometer Figure 1.20c shows a chip which can perform the following functions: optical buffering, differential phase-shift keying (DPSK) de-

modulation, intensity modulation, and differential XOR logic operation [73]. By properly controlling the current supplied to the active elements in the circuit loop (i.e. a semiconductor optical amplifier and a variable optical attenuator), the relative phase of the propagating signals can be adjusted, changing the interference condition between the input signal and its delayed copies. In buffer configuration, up to 13 circulations (corresponding to a 1.62 ns delay for 12.5 Gb/s data) are demonstrated. Used as DPSK demodulator no significant BER power penalty is observed for 8 Gb/s signals, compared to a thermally tuned commercial demodulator. Error-free operation for a 1-, 2-, and 4-bit differential XOR logic gate has been demonstrated at 8, 16, and 32 Gb/s, respectively.

4 × 4 Space and Wavelength-Selective Switch Figure 1.20d shows a four input four output space and wavelength selective cross-connect [74]. The circuit is implemented with 32 SOA gate switches and four cyclic 4 × 4 AWG routers with a nominal 400 GHz wavelength channel spacing. This allows for the arbitrary and fast reconfigurable connection of wavelength channels from each input to each output. The circuit is the first in class for simultaneous wavelength and space selective routing. Multi-path routing was performed with both co- and counter-propagating data. Bi-directional and fast reconfigurable routing has similarly been quantified to show low power penalty of less than 1 dB for the simultaneous routing of data over multiple circuit paths.

16 × 16 Photonic Switch Figure 1.20e shows a monolithic sixteen input, sixteen output photonic switch which is designed for broadband photonic packet-routing [33, 75]. The circuit is constructed as a hybrid Beneš architecture in three stages, with arrays of 2 × 2 switch building blocks at the inputs and outputs, and a centre stage implemented with an array of eight 4 × 4 switch building blocks. Switching within each of the building blocks is implemented by broadcast and select: The broadcast is facilitated with 288 multimode interference (MMI) splitters, and the select function is implemented with 192 SOA gates. With a total of 480 components integrated on a single chip this is one of the largest PICs reported so far. The use of low loss passive waveguides in combination with high contrast active gates leads to promising system level metrics in terms of optical signal to noise ratio and electrical energy use [33]. Multi-path dynamic re-configuration is enabled through the connection of the circuit to programmable logic [75].

Broad Frequency Comb Laser Figure 1.20f shows a mode-locked ring laser with a very wide comb spectrum [76]. The laser consists of straight and curved waveguides, an SOA section, a saturable absorption element, electrical isolation sections and a 2 × 2 MMI coupler. The SOA element, which provides optical gain, was divided into two sections of equal length (345 μm) with a 30 μm long saturable absorber in between. For the SA a short reverse biased SOA section was used. The laser was operated by reverse biasing the SA and forward biasing the SOA sections. It features a 20 GHz comb spectrum with FWHM bandwidth of 11.5 nm (1.41 THz) and 17 nm (2.16 THz) when measured at -10 dB. These are record values when compared to the results obtained from devices with a similar geometry based on QW material.

1.6.2 Oclaro Platform

Oclaro has been involved from the beginning in the ePIXnet initiative for the introduction of a foundry model into photonic integration. It is participating in the JePPIX

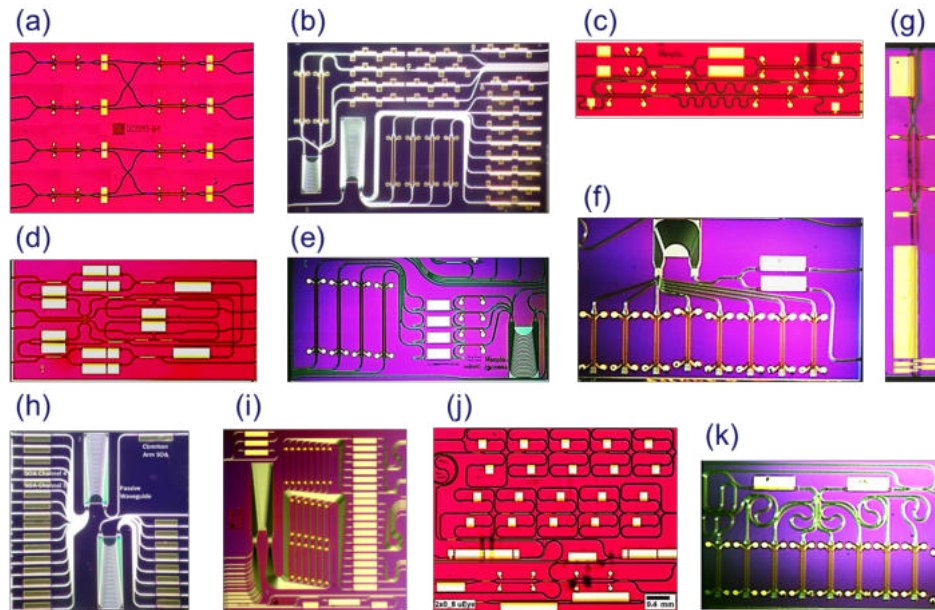


Figure 1.21: Examples of Photonic ICs realised on the generic Oclaro platform. a) Low energy optical switch; b) PIC with a 4- and an 8-channel WDM transmitter. The 8-channel transmitter integrates 74 components on a chip area of $3 \times 5 \text{ mm}^2$; c) a $1 \times 4 \text{ mm}^2$ InP 'all optical' transmultiplexer chip; d) Widely tunable laser chip; e) Filtered-feedback multi-wavelength transmitter ($2 \times 4 \text{ mm}^2$); f) 8-channel WDM reflective modulator with dimensions $3 \times 2 \text{ mm}^2$; g) Pulse laser with tunable repetition rate; h) AWG-based multiwavelength laser used for TeraHertz generation by mixing of two channels; i) Pulse shaper for bio-imaging integrating a 20-channel AWG with 20 SOAs and 20 phase modulators. The chip measures $6 \times 6 \text{ mm}^2$; j) 10-bits Switched delay line. The chip measures $4 \times 6 \text{ mm}^2$; k) 8-channel pulse serialiser containing 2 SOAs, 8 MI-modulators and 7 delay lines.

platform. For its commercial products Oclaro has developed a technology for integration of tunable DBR-lasers with MZI modulators [77]. This technology offers high performance SOAs, tunable DBR gratings and phase modulators. In the EuroPIC project Oclaro worked on preparing this technology to support a broad range of functionalities in both telecom and non-telecom applications. In the PARADIGM project it has worked on further extension of its capabilities to 40 Gb/s full transmit and receive functionality. Below a number of examples are given of experimental ASPICs that have been realized in Oclaro's first generation generic platform technology. The chips have been developed in the framework of the EuroPIC project and the Dutch MEMPHIS project. In 2016 Oclaro stopped offering open-access foundry service.

Low energy scalable high speed optical switch Figure 1.21a shows a chip containing 2×2 port building blocks for an ultra-low energy scalable high speed optical switch [78]. This device comprises both Mach-Zehnder modulators and semiconductor optical amplifiers (SOAs) to optimize switching energy and performance in nanosecond switching time lossless switches for data centre and internet switching and routing applications. The component has very low power penalty. After 3 cascades which would emulate an 8×8 port switch, the eye diagram shows almost no impairment. Input power dynamic range is 14dB for a 0.5 dB penalty. The switch does not require 50Ω

matching resistors which dramatically reduces its electrical power consumption. This is all predicted to result in a 95% power reduction compared to a conventional SOA switch.

WDM transmitter Figure 1.21b shows a WDM transmitter for use in the Central Office of a FTTH network [68]. The transmitter chip contains an array of DBR-based lasers and Mach-Zehnder modulators. It is designed for transmitting four modulated downstream (DS) data channels and four CW signals on which the upstream (US) data can be modulated at the subscriber using a reflective modulator. An AWG is used to multiplex all the optical signals into one common output waveguide. The transmitter is designed to operate at a 100 GHz wavelength grid at 1550 nm. It delivers up to 4 dBm of optical power/channel into the fibre with a modulation data rate of 12.5 Gbps per channel.

WDM-TDM Transmultiplexer Figure 1.21c shows the first integrated all-optical WDM-TDM multiplexer, for wavelength grooming of a number of WDM channels into a single TDM channel at the aggregate line rate [79]. For design and mask layout of the Mux circuits, simple equivalent circuits were developed, representing the incorporated wavelength converter. With the realized chips, successful WDM to TDM transmultiplexing was demonstrated from 2×10 Gb/s WDM to 1×20 Gb/s TDM, as well as multiplexing of clock and NRZ data to narrow pulse RZ data.

Widely tunable laser Figure 1.21d shows a new widely and continuously tunable ring laser [69]. The chip combines two gain sections with an integrated, tunable 4th order series filter with a Vernier pair of Ring Resonators (RR) and a pair of identical Delayed Interferometers (DI). With an identical and optimized phase shifter (in forward bias: $\sim 90^\circ/\text{mA}$) in all RRs and DIs, tuning currents of only a few mA yield tuning ranges of 2000 GHz. Vernier pairing of the DIs doubles this continuous tuning range to 4000 GHz.

Filtered-Feedback Multi-Wavelength Transmitter Figure 1.21e shows a filtered-feedback multi-wavelength transmitter [80]. The laser consists of an array of FP lasers, each of which is formed by a semiconductor optical amplifier (SOA) and two on-chip broadband MMI Reflectors (MIRs). One side of each FP laser is coupled to an AWG filter through a phase shifter. The AWG acts as a wavelength filter outside the laser cavity, and its output port is connected to another MIR to provide feedback. The phase shifting sections can adjust the phase of the feedback signal to optimize the stability of the laser. This laser can operate with four channels simultaneously. Each channel has stable single mode lasing with an SMSR better than 40 dB. The filtered feedback reduces the laser linewidth to 150 kHz. The outputs of the laser channels are routed to 1 mm long MZ modulators on the same chip.

8-Channel WDM Reflective Modulator Figure 1.21f shows an 8-channel WDM reflective modulator using Michelson-Interferometer Modulators [81]. Measured bandwidth of the Michelson modulators is > 18 GHz. Eye-diagrams for 12.5 Gb/s signals in back-to-back configuration are wide open with a dynamic extinction ratio of 10 dB. Transmission experiments through 85 km of SMF fiber showed error-free operation at 10 Gb/s.

Pulse Laser with Tunable Repetition Rate Figure 1.21g shows a mode-locked pulse laser operating at 14.4 GHz monolithically integrated with a pulse-picking Mach-Zehnder modulator for reducing the pulse rate and an SOA for increasing the output power [82]. The laser generates 12.5 ps pulses. The Mach-Zehnder modulator allows tunable repetition rates from 14 GHz to 109 MHz, and the SOA boosts the peak power by 3.2 dB. The device approaches performance figures suitable for biophotonic applications in a compact and cost effective platform.

Dual Wavelength laser for THz generation Figure 1.21h shows an AWG-based multi-wavelength laser which is used for generation of a 95 GHz carrier frequency by optical heterodyning of two wavelengths from adjacent channels of the AWG-laser. The extended cavity structure of the device provides low phase noise and narrow optical linewidth, further enhanced by the intracavity filter effect of the arrayed waveguide grating. The generated RF beat note, at 95 GHz, has a -3 dB linewidth of 250 kHz. This is the narrowest RF linewidth generated from a free-running dual-wavelength semiconductor laser [83].

Pulse shaper for bio-imaging Figure 1.21i shows an integrated pulse shaper with a reflective geometry [84]. The photonic integrated circuit combines a 20-channel AWG-filter with 50 GHz channel spacing, 20 electro-refractive phase modulators (ERMs) and 20 semiconductor optical amplifiers (SOAs). The light from the optical pulse source, i.e. a mode-locked laser, is divided into twenty spectral components by the AWG. The ERMs and SOAs are used to manipulate the spectral phase and amplitude of the components in order to achieve the desired pulse shape. The spectral components are then recombined in the AWG. The integrated pulse shaper is used to demonstrate chirp compensation for the pulses from a mode-locked quantum dash laser diode. Reduction of the pulse width from 7 ps to less than 3 ps is demonstrated.

Ten-bit Switched Delay Line Figure 1.21j shows a photonic 10-bits switched delay-line circuit for use in a BOTDR strain sensor system [85]. The circuit consists of a chain of delay elements. In each delay element light is split over two optical paths by an MMI-splitter. Each path contains an SOA that can be operated as a gate switch: either blocking or amplifying the light. By controlling the SOAs light can be selected from either the longer or the shorter path of the delay element. The optical path of the whole chain consists of 10 switchable delaying elements with length ratios 1,2,4, . . . , 512 and it can be tuned over 1024 different delay values.

8-Channel Pulse serialiser Figure 1.21k shows an 8-channel integrated photonic pulse serialiser with dimensions 3×2 mm² [86]. The chip is designed as a data read-out unit for the KM3NeT Neutrino Telescope which is planned to have 186,000 Photo-Multiplier Tubes that have to be read out every nanosecond. The ASPIC architecture consists of a distribution network with 1×2 MMI power splitters and optical delay lines for multiplexing of optical pulses in the time domain, Semiconductor Optical Amplifiers for loss compensation and reflective amplitude modulators in Michelson Interferometer configuration for data encoding. A static extinction ratio of over 12 dB was measured. The distribution network provides accurate time delay and multiplexing of the 1 Gb/s readout signals on a 32 Gb/s output signal.

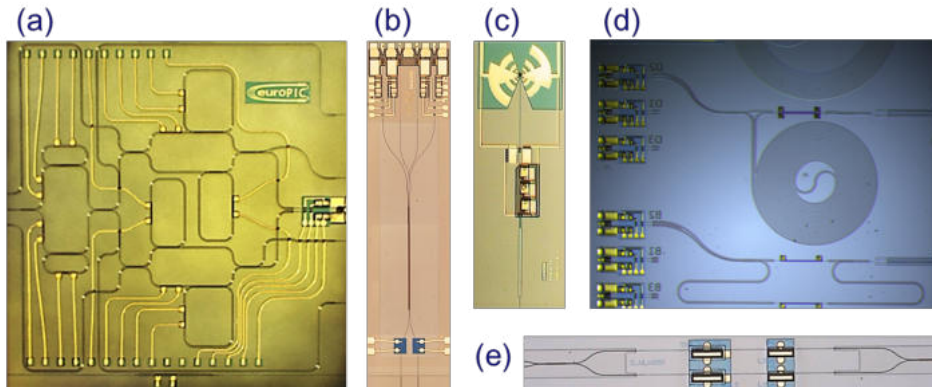


Figure 1.22: Examples of Photonic ICs realised on the generic Fraunhofer HHI platform. a) Frequency discriminator chip containing MZI structures coupled with ring filters and balanced photodiodes; b) Integrated QPSK receiver chip; c) Opto-rf converter for sub-THz applications; d) Read-out chip for a 4-channel FBG strain sensor; e) Transmitter for cw THz applications implemented on HHI's extended Tx/Rx integration platform.

1.6.3 Fraunhofer HHI Platform

Fraunhofer HHI has developed a technology for fabrication of high speed receivers, the key element of which is a high-speed waveguide integrated pin photodiode [87]. It is commercially exploited by u2t Photonics (www.u2t.com), a spin-off company of HHI. This technology offers high performance balanced detectors and their integration with passive components and spot-size converters. In the EuroPIC project HHI has been working on preparing this technology for supporting a broader range of applications in a foundry setting. In PARADIGM it has worked on further extension of its capabilities to full 25 Gb/s transmit (Tx) and 40 Gb/s receive (Rx) functionality. Below a number of examples are given of experimental ASPICs that have been realized in HHI's generic platform technology. The chip shown in Figure 1.22e has been realized on the new Tx/Rx platform.

Integrated Frequency Discriminator Figure 1.22a shows an integrated frequency discriminator for application in phase-modulated microwave photonic links [88]. It contains a cascaded structure of lattice filters realized by ring-loaded MZIs to result in an IIR-equivalent optical filter. An input filter splits the spectrum of the FM optical signal into two separate bands each of which is fed into a filter providing a linear ramp in intensity. Finally, both bands are detected in a balanced detector. Comparison of experimental and simulated filter characteristics already indicates good agreement for this first fabrication run. The discriminator exhibits SFDR values between 67 and 79 $\text{dB} \cdot \text{Hz}^{2/3}$ or signal frequencies in the range of 5-9 GHz, basically limited by the experimental test setup. We expect that values in the range of 104-116 $\text{dB} \cdot \text{Hz}^{2/3}$ will be achievable.

Integrated QPSK receiver Figure 1.22b shows a receiver chip for the detection of 28 Gbaud QPSK transmission signals [89]. Its central element is the 90° hybrid mixer implemented in the form of a 2×4 MMI coupler. This coupler is connected to two pairs of waveguide-integrated dual photodiodes for the I and Q channels. Waveguide crossings

are used in the output network to fulfil the phase relationship between the neighbouring diodes. The input waveguides provide mode expansion (SSC) enabling coupling loss as low as 1 dB to SSM fibres. Responsivity of the device shown is close to 0.1 A/W over the C-band, with CMRR values of -10 dB in the worst case.

Opto-rf converter for sub-THz generation Figure 1.22c shows an integrated chip that comprises a high-frequency photodiode coupled with a logarithmic periodic antenna [90]. The photodiode itself can be remotely biased by three other photodiodes connected in series with it and optically powered via the input fibre and an on-chip 1:4 MMI power splitter, thus avoiding any external electrical biasing. The antenna converts high-frequency optical signals into microwave/sub-THz radiation. Launching light from a tunable heterodyne laser source into the device, radiated power in the 1-digit μ W range at around 5 mA of photocurrent was obtained in the frequency range up to 400 GHz.

Read-out chip for 4-channel FBG strain sensor Figure 1.22d shows two wavelength meters on a chip with fibre matched spot-size converters. The devices measure a wavelength shift in a fibre Bragg grating, anywhere in the 1465 to 1620 nm window [91]. Each device has a 1×2 Mach-Zehnder Interferometer and the signals from the outputs of the 2×2 MMI in each MZI are fed into a balanced detector. The wavelength meters have a FSR of 10 pm and 100 pm, using an integrated spiral delay line with 64 mm length for the 10 pm FSR. The responsivity of a packaged device is 0.29 A/W. A subfemtometer resolution is feasible at a sampling rate of 10 kHz and -10 dBm fibre power. This is several orders of magnitude better than commercially available small-sized wavelength meters.

Transmitter for THz applications Figure 1.22e shows a photonic integrated circuit designed for continuous wave THz generation [92], which has been fabricated during trials of the new HHI Tx/Rx platform. Two wavelength-tunable DFB lasers are incorporated into an MZI structure together with current injection based optical phase modulators and MMI couplers. This chip provides full control of the THz signal by using a unique bidirectional operation technique. Integrated heaters on the laser elements allow for continuous tuning of the THz frequency over 570 GHz. Applied to a coherent cw THz photomixing system operated at 1.5 μ m optical wavelength, a signal-to-noise ratio of 44 dB at 1.25 THz was reached, which is identical to the performance of a standard system based on discrete components.

In chapter 27 we will elaborate a number of PIC designs in more detail.

1.7 ASPIC Design Environment

The introduction of the generic foundry approach in photonics will cause a major change in the sophistication of photonic chips: it will move the design from a device level to a circuit level, a move that occurred in microelectronics in the '70-s and '80-s, and that is now happening in photonics too.

In the generic approach a high performance standardized process is accessible via Process Design Kits (PDK) with a number of building blocks, the performance and functional behaviour of which is accurately known. Designers do not have to be concerned about how to design them, they can just take them from a library and start building a

circuit and analyse and optimize it with a circuit simulator. Of course a good knowledge about the operation of the building blocks is still important, but detailed knowledge about the process technology and the layer stack is no longer required. Therefore the designer can concentrate on a higher abstraction level of circuit design. Just like system designers that build their circuits from discrete optical components, of which they know the behaviour, but not what's exactly inside the box. ASPIC design is very similar, but now the system is integrated on a single chip. Further the designers have some additional freedom because a number of the building blocks are parameterized, so that they can adapt their performance to specific requirements, which is not so easy with discrete components, where only a limited number of different types will be available.

We will briefly describe what the Design Environment for a generic process looks like.

1.7.1 Software Environment

The Software Environment contains the required software tools; these include not just circuit simulators and mask layout tools, but also physical modelling tools such as mode-solvers, BPM, EME or FDTD tools, non-linear time domain models, electrical and thermal simulators. All or any of which may be required for performing simulations on a sub-circuit or device level.

Physical simulators

Physical simulators analyse the behaviour of optical and/or electrical structures and components using electromagnetic modeling. They may include thermal or acoustic modeling. For Integrated Photonics mode-solvers are the most elementary category: they can calculate the properties of guided and radiating modes in two-dimensional (2D) structures. For 3D structures more complex tools are required to analyze the field propagation and scattering, they can be based on Finite Difference Time Domain (FDTD) or Beam Propagation Methods (BPM). Including also electrical effects like current injection, modulation signals and detected signals adds another level of complexity to the design tools. There is a large variety of Physical Simulators. A brief description is given in Chapter 7.

Circuit simulators

Circuit simulators sit one level above physical simulators. They make the assumption that the light is flowing in clearly defined waveguide modes. This allows them to simulate much larger circuits than a physical simulator could. Circuit simulators work with so-called compact models of the actual components making up the circuit – i.e. models that give the correct behaviour (within defined limits) but using simplified mathematical models that can be evaluated quickly.

Within the JePPIX consortium four circuit simulators are used: Aspic™ from Filarete for linear wavelength domain simulations, PICWave from Photon Design for non-linear time domain simulations, VPI for circuit simulation in both the wavelength and the time domain, and ADS, Agilent's Advanced Design System for optical, RF, microwave and high speed digital applications. ADS offers a very powerful simulation and parameter extraction engine, which it is not (yet) commercially supported for photonic design, however. We will give three examples of circuit simulations that illustrate their potential for Photonic IC design on the JePPIX InP platforms (Oclaro, Fraunhofer HHI, SMART Photonics/COBRA). A more extensive description is given in Chapter 7.

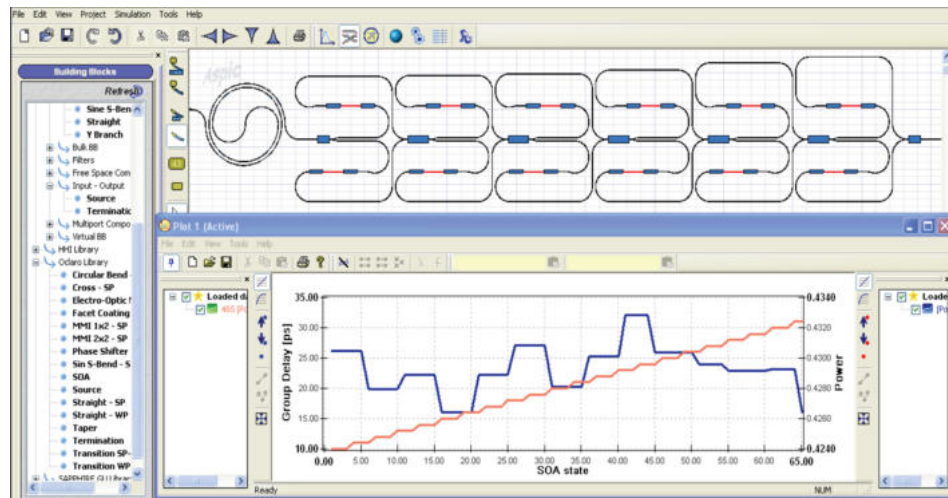


Figure 1.23: Screenshot of the Aspic™ simulator output with the circuit to simulate at the top and the plot window with the simulation result at the bottom.

Aspic™ (Filarete) Aspic, Advanced Simulator for Photonic Integrated Circuits [93], is a frequency domain circuit simulator for passive linear PICs. Each building block is described by analytical models and numerical data embedded in scattering matrices. Models can be either derived from the theoretical behaviour of the building blocks or can be built through electromagnetic simulations, and can also include experimental data. Foundry based models containing the realistic description of building blocks fabricated by several photonic foundries (e.g. HHI, COBRA/SMART for InP technology and Lionix for TriPlex) are available and organized into specific libraries.

Arbitrarily complex PICs can be designed by combining a large number of basic and composite BBs included in the BB libraries. To perform the simulation, Aspic™ assembles the scattering matrices of all the BBs of the circuit and provides amplitude, phase, group delay response, and chromatic dispersion at the input/output port of each BB (forward and backward field). Scan and sweep operations versus any geometrical or optical parameter of the circuit can be performed as well. Once the circuit is optimized by the user, it can be directly exported to a mask layout editor (MaskEngineer) .

Large flexibility in the choice of the BB parameters makes the user do much more than a simple spectral analysis, enabling for instance “what if” analysis, virtual experiments, tolerance analysis, case analysis, statistical analysis based on Monte-Carlo simulations to evaluate the robustness of the circuit against fabrication uncertainties, and so on. Figure 1.23 shows a typical screen shot of the simulator. It shows a discretely tunable delay line used in one of the ASPICS discussed in the previous section [85]. It is based on a split and select technique with SOA gates. The state of each SOA is defined by its electrical current, which is loaded from a text file, and the spectral response is simulated for each state. The output power and the group delay at a given wavelength are shown in the plot below. The simulation of this rather big circuit requires just a few seconds to be performed, a result not achievable with electromagnetic simulations.

PICWAVE (Photon Design) PicWave is a time-domain based photonic circuit simulator that is capable of modelling both passive and active components. Passive (linear components) can be specified by simple parameters like the optical length of a waveguide, or the coupling coefficient of a directional coupler; or alternatively a wavelength-

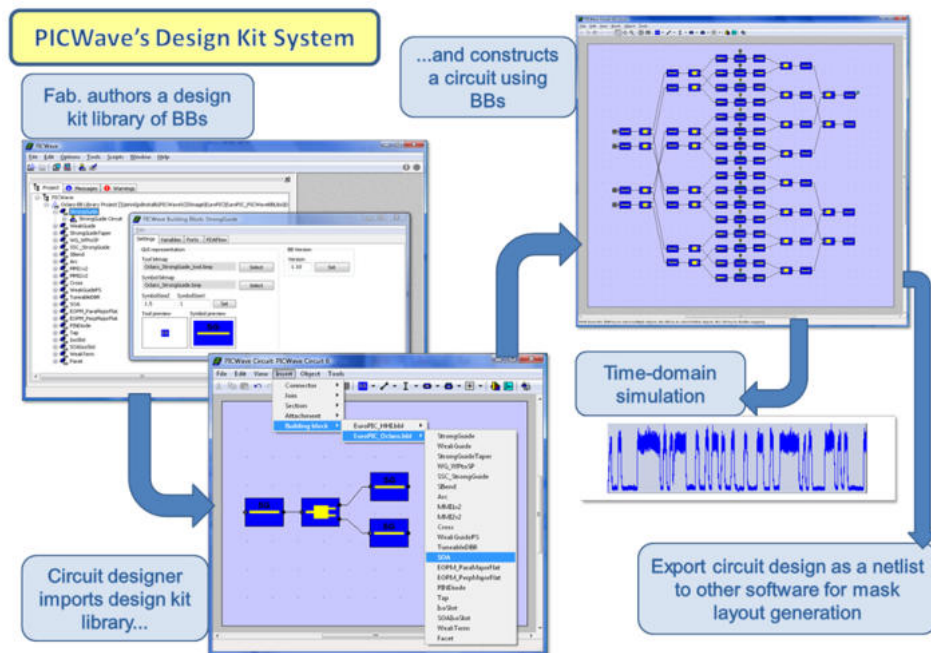


Figure 1.24: Design flow based on PICWave circuit simulator.

dependent S-matrix. PICWave also has detailed models of active components such as semiconductor optical amplifiers, laser diodes and optical modulators. In contrast to passive components, where good surrogate models like the S-matrix formulation exist, it is difficult to create simple surrogate models, of an SOA for example, that match static and dynamic characteristics over a large operating range of temperature, electrical drive, optical input etc., at all modulation rates from MHz to 10's of GHz. Thus the PICWave active models include a lot of relevant physics such as carrier diffusion, spatial hole burning and current spreading.

Design kits using PICWave can provide the designer detailed models of their active building blocks that behave correctly over a wide range of operating conditions. This allows even the inexperienced circuit designer to include complex components like SOAs into a design without having to be an expert in optoelectronics modelling.

ADS (Agilent) Agilent's Advanced Design System is an electronic design automation software tool for RF, microwave, and high speed digital applications. By adding custom modules it becomes possible to use ADS also for simulating complex Photonic ICs [94]. COBRA has added many components ranging from single and multi-mode waveguides to MIRs and AWGs. The models employ an effective index based mode solver, and the simulation results are, therefore, firmly based on the physical properties of the circuit. With this approach, it is possible to see how the circuit responds to variations in etch depths or waveguide widths. Figure 1.25 shows a symbolic view of a PIC in ADS. The circuit consists of an AWG with one output channel connected to a Fabry-Perot cavity created by cascading two MIRs. The inset shows the simulation results, and the AWG channels plus the Fabry-Perot response can be clearly recognized.

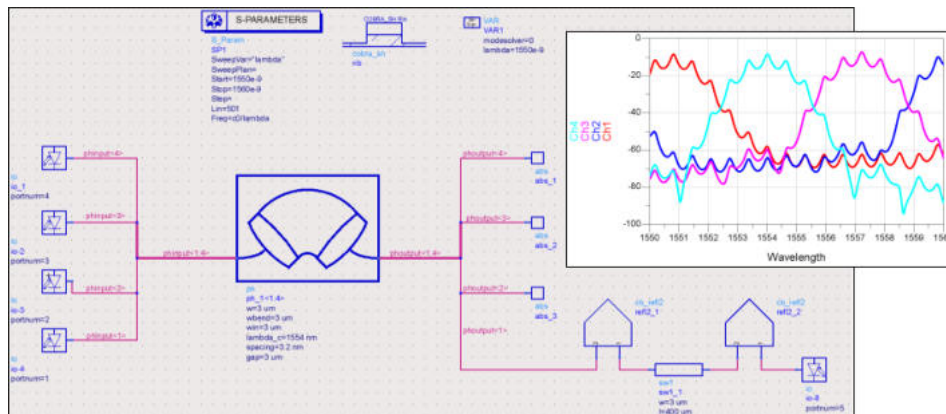


Figure 1.25: Circuit schematic in ADS of an AWG connected to a Fabry-Perot cavity. Inset: wavelength response of the circuit.

Mask layout tools

After a circuit has been designed and optimized we want to validate conformity to the design rules of the foundry and generate the mask layout. The JePPIX consortium is working with Nazca Design, Mask Engineer from Phoenix Software (now Synopsys), and Luceda Photonics. Once a satisfactory design has been created with a specific foundry and package in mind, it can be transferred to a mask layout.

With the mask layout software, it can be further completed and optimized (which is necessary because the circuit simulators cannot generate the full circuit mask layout) after which the PIC design is translated into GDSII or OASIS (binary) mask files. During this process, automatic data processing takes place that obeys design rules set by the foundry. For example, a waveguide may have to be wider on the mask than in the original design in order to compensate for a known amount of under etch. Or the definition of a waveguide may involve a local mask inversion. In addition, the software will perform foundry specific design rule checks (DRC) at the logical and mask levels. The design can, for example, be checked for rule compliance on the minimum allowable bend radius, or a check may be performed to ensure that metallization and waveguide layers are neither overlapping nor closer than a minimum distance. All the building blocks are defined with stay out regions called bounding boxes to avoid overlaps and proximity effects in the InP process. Figure 1.26 gives an example of a mask layout element (a curved connector) and a mask layout view.

When the PIC design is part of a Multi Project Wafer (MPW) run, a brokering organisation (like JePPIX) or the foundry will collect the mask files from all participating users and place them in individual reticle cells. When the mask set is ready, the wafers can then be processed by the foundry. If IP-protected or “private” building blocks⁶ are used, the foundry will replace their bounding boxes with the actual mask layout. The foundry may also add process control features, alignment and cleaving marks, for example in the final stage of mask assembly.

A foundry can make available unique building blocks that are covered by patents or trade secrets. The unique building block may contain IP owned by the foundry, one of the software tool developers or other designers and released for general use under

⁶The IP-protected building block is any building block which has IP-protection. As the Basic Building Blocks are automatically licensed to the user by the foundry, IP protection is most relevant for Composite Building Blocks. So in practice an IP-Block is a CBB with IP-protection.

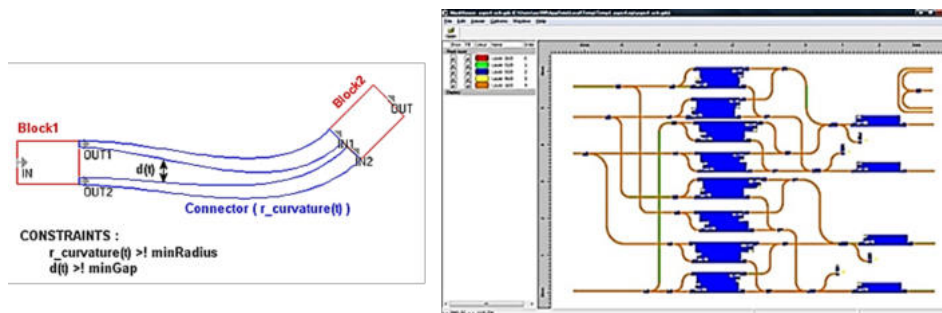


Figure 1.26: Example of a mask layout element and a mask layout view in Mask Engineer.

license. These BBs are represented by a bounding box in the design kit that hides what is inside the box, but does detail the location of input and output waveguides, electrical connections as well as the functionality of the building block through a wavelength dependent scattering matrix or other models.

The API is an essential part of a horizontal development business model where independent companies provide different elements of a technical solution. Through standardisation initiatives, such as those of openEPDA and PDAflow⁷, the interfaces in a horizontal model between layers, be it software or technology, are well defined and accessible to developers and licensed users. It makes the system flexible to gradual upgrades and competition. IP-blocks in such a system can be used by developers and, very importantly, also licensed to outside users either individually or through support contracts, if desired.

1.7.2 Design Manual

The Design Manual is a document that contains the information needed by a user to design an ASPIC on a platform. It can be provided directly by the InP foundry, but usually it is distributed through a brokering organization (JePPIX for the InP platforms). All relevant technical information about the building blocks that are available within the developed generic technologies at the foundries is consolidated into the Design Manual which describes the complete generic platform offering including information on the available chip sizes, packages and the use of the software tools.

1.7.3 Process Design Kit (PDK) and Component Libraries

The Process Design Kit or PDK is a (licensed) plug-in library for the Software Environment containing the technology and/or foundry specific technology information such as set-up files for mask layer information, building blocks, design rules and design rule checking. The PDK may also contain layout information and templates for standardization of optical and electrical port positions. It is the responsibility of the foundry to ensure that it is correct and up to date.

An important part of the Process Design Kit is the Component Library. It contains the mask layout and a model description of a number of building blocks. The PDK may contain a number of component libraries owned by different parties, but provided by the broker or the foundry.

⁷Specifications are found at <https://openEPDA.org> and <http://PDAflow.org>.

The Component Library contains as the most basic part a set of Basic Building Blocks. The foundry may decide to make additional building blocks with higher complexity (Composite Building Blocks) also available to the PDK users, on conditions to be determined by the foundry. In addition designers may also develop their own building blocks (CBBs; BBBs can be provided only by the foundry) and make them available to other designers via the PDK, or directly to the interested users. The conditions for using these can be chosen by the owner of the building block.

The component library enables the designer to use components (building blocks) without knowing all the details about their operation and fabrication. The potential of a foundry process is determined by the performance, but also by the number of building blocks that are available in the library. A foundry platform with a library containing a variety of well-defined building blocks for MMI-couplers, AWGs, amplitude, phase and frequency modulators, including complex modulators like DQPSK and PM-DQPSK modulators, SOAs, CW and pulse lasers with varying pulse widths and rates, tunable and multi-wavelength lasers, fast switches, wavelength selective switches, polarization converters, splitters, combiners and controllers, will cause a revolution in the way in which complex photonic ICs will be developed. Furthermore, once a building block is available designers can start to expand its application to even better performance, higher accuracies, more ports or more wavelengths, larger wavelength ranges, to mention just a few possibilities.

Creating accurate basic or composite building block descriptions for the component library is a major effort. It requires a thorough analysis and optimization of the component and extensive characterization and testing in order to provide an accurate prediction of its performance. It will require an army of researchers for developing all those building blocks, but once we have a good library it will speed up the development of Photonic ICs by at least an order of magnitude and reduce the design cost accordingly.

The two main components of a building block description in the library are the mask layout and the model description.

The mask layout contains the layout information for all the mask layers that are used in the fabrication process. The designer can choose the position on the mask where to include the component, and the orientation of the component in the circuit. If the component is parameterized the designer can choose the value of a geometrical parameter (e.g. waveguide width, bending radius, section length of SOAs or Phase Modulators) or even an optical parameter for more advanced building blocks (like free spectral range for an AWG) within the design rules, which usually set limits on the range of possible values. The applied building block contains the detailed layout information, but as discussed earlier it may also show up as just a symbolic layout block which shows the position and the size of the component, including the location of the input and output ports for both the photonic and electric connections. For such protected or “private” building blocks the detailed information is inserted by software owned by the foundry before the masks are fabricated. In this way, IP of the owner can be effectively protected. If the library provides a good model description of the building block the designer is not hindered by lack of knowledge of exactly what’s inside the box.

So far mask layout can be generated either directly in the layout software or through a circuit simulator. Optimisation of the layout for minimal area usage and/or RF constraints is still required in the layout software. Longer term, auto-layout of a whole circuit starting from a symbolic circuit description may become feasible. But at the moment the interconnect problem (routing) has too many degrees of freedom and is too complex to be solved automatically. A number of semi-automatic interconnect tools are available to support the designer with this job.

The model description in its simplest form can be a written description of what a building block does, supported by some measured data on its performance. Research is ongoing for developing software descriptions for the PDKs that can be used in connection with the circuit simulators. The most straightforward way to do this, at least for linear components, is by providing an S-matrix to the circuit simulator which describes the coupling between the different ports. In a more sophisticated form the S-matrix elements may be specified as a function of wavelength, polarisation or waveguide mode. The model may contain a description of non-linear behaviour of the materials inside the component, including effects of injected carriers. Doing this for all components described chapters 8-24, for all the platforms, is a huge effort which will take many years for many researchers, but it is key to the future application potential of the platform. Within the PARADIGM project a significant effort has been made towards creating building block descriptions for a number of passive devices and lasers. Since the benefit of this effort is shared by the end-users, a large cost reduction is achieved compared to traditional in-house development approaches.

1.8 Generic Packaging

Integration is critical in reducing the number of packaged parts, and thus reducing sub-system cost, as evidenced by the acceptance of extensive integration in the emerging generation of 100Gbit/s transceivers. In a generic foundry approach the costs of small and medium size chips are expected to drop below one hundred Euros already for small volumes. With such low chip costs the total costs of a module will be dominated by the package. Packaging technologies require, therefore, a comparable generic approach to ensure sustained cost reductions over time.

The normal procedure for photonics packaging (unlike microelectronics packaging) is to design a bespoke package to suit the chip with minimal attention to using a truly standard package. In a generic approach this process is reversed: a versatile standardized generic package is developed and the chip has to be designed such that it complies with the standard package. Such an approach requires standardization of the chip size and the optical and electrical interfaces. This means a paradigm shift in photonic packaging.

As it will not be possible to develop a single package that covers all possible ASPICs, the approach in generic packaging technology so far has been to develop a small set of packages that can be used for a large number of different ASPICs, e.g. a package that can handle up to ~ 10 optical IO-ports, a large number of electrical dc ports (e.g. 40) and 10 RF ports, and one or two packages for smaller port counts. As an example we describe part of the work that has been done in the PARADIGM project.

1.8.1 A standardized Package.

The need for standardisation of critical high volume high performance packaging has been recognised by the IEC, the International Electrotechnical Committee who have standardized the ROSA (receiver optical sub assembly) and TOSA (transmitter optical sub assembly) package formats used in many high speed transceiver products used in high volume for both datacom and telecom applications. These two packages are then combined to sit side by side in the transceiver. For the large ASPICs with enhanced functionality offered by PICs fabricated on a generic platform it is sensible to combine the footprint of the TOSA and ROSA to produce a single package capable of fitting within the standard transceiver package body.

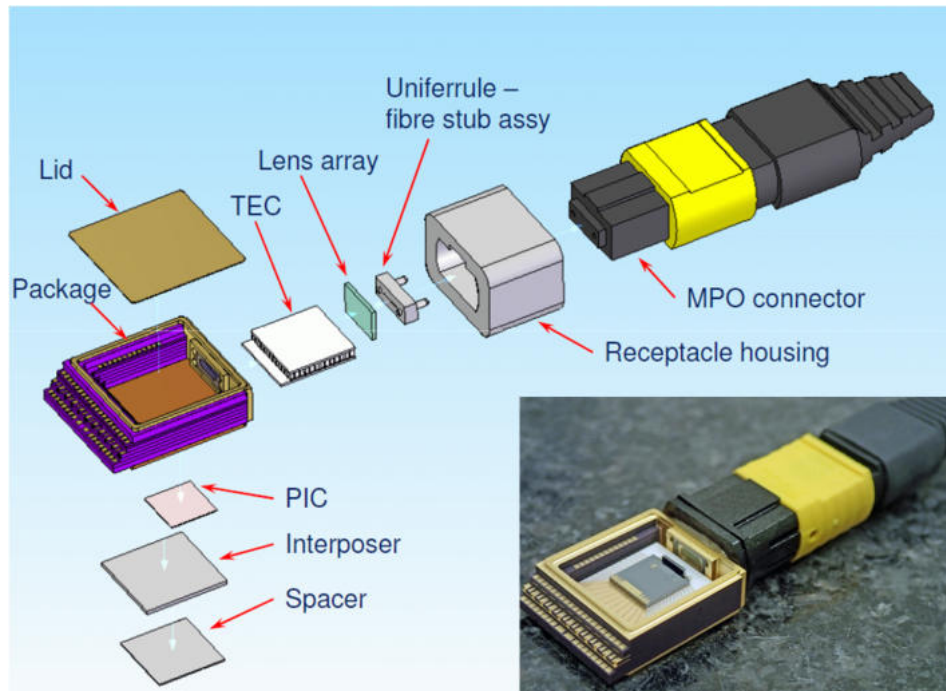


Figure 1.27: Exploded view of POSA package. Inset: test chip with lens array mounted in POSA package.

The package is designed with the following features:

- Standardised package format (potential IEC adoption)
- Up to 12 optical input ports
- Up to 10 RF ports with 25 GHz bandwidth
- Up to 36 DC ports and high-current TEC connections
- Captures connectivity requirements for more than 80% of PIC designs so far in MPW runs.
- XFP and other electronics package compatible
- TEC support
- Flex PCB / lead frame / wire bond interface
- Pigtail and optical connector compatible

This new POSA (PIC Optical Sub Assembly) measures just $15.5 \times 18 \times 5$ mm, with an internal active device cavity ~ 10.5 mm square. The package has been designed in conjunction with one of the largest manufacturers of this style of package to ensure the highest performance, best price and manufacturability. This will ensure compatibility with many high volume ROSA and TOSA manufacturing lines and also with typical prototyping capabilities associated with many foundries. All of these factors should help minimise cycle times for new products with the best cost.

1.8.2 A standardized Chip

To comply with a standardized package the optical and the electrical interfaces of the chip have to be standardized too, as well as its form factor. With the freedom that is offered to designers in positioning their components on the chip, it has turned out that fixing the positions of the optical input and output ports is not a large constraint, designers found it easy to comply with this standard. The requirement may introduce some additional waveguide length in the chip, but with a clever design this will be of order of a few mm maximum. Additional propagation losses in a low loss process are small.

Standardization of optical interfaces. For the optical ports the most important features of a standard for multi-port interfaces are the spot size of the optical ports and their pitch. For direct coupling to a fibre ribbon a spot size of $\sim 10\ \mu\text{m}$ and a pitch of $250\ \mu\text{m}$ are required. The Fraunhofer HHI (receiver-type) platform has a Spot Size Converter (SSC) with such a large output spot. But for platforms that also include lasers and amplifiers enlarging the mode to such a diameter significantly complicates the process technology. The Oclaro (transmitter-type) platform has an SSC with a $3\ \mu\text{m}$, circular, output spot. This is considered a good compromise between integration process complexity and packaging complexity and it is adopted as a provisional standard within the JePPIX consortium. For the pitch an integer multiple of $25\ \mu\text{m}$ is agreed. This is compatible with the $250\ \mu\text{m}$ pitch of fibre ribbons, but it also allows much denser spacings which can be realized when coupling the chip to a high-contrast dielectric interposer chip. In order to support angled facets without having to rotate the optical chip special features are included in the chips in order to have a straight output beam also for angled facets.

Standardization of electrical interfaces is quite common in microelectronics. The most common approach for the dc-contact is to bring them to the edges of the chip and agree on size and pitch of the bond pads. This requires an interconnect plane that can cross the optical waveguide layer. The Fraunhofer HHI, COBRA and Oclaro platforms all offer this facility. For the rf-ports standardization is more complicated. For bringing the contacts to the edge of the chip an rf-interconnect plane with low rf losses would be required. This is not yet available in any of the JePPIX platforms.

Standardization of chip size. For the chip size a standard of 2, 4 or 6 mm for both dimensions of the chip has been agreed. This will reduce the number of different interposers that are required between the edge of the chip and the edge of the package.

In chapter 26 we will describe in more detail packaging standards and design for packaging.

1.9 Generic Testing

1.9.1 Wafer Validation

In a generic process the performance of the process has to be validated for each wafer run; the customer will expect such a validation. Validating the process on the performance of user ASPICs is not practical in an MPW run; each ASPIC will require a different test setup and procedure, and failure of the ASPIC does not mean that the process failed, the problem can also be in the user design. The only practical way for validating a generic process is by including a test cell for the characterization of the basic building blocks. If the performance of the BBBs is OK, the performance of all components that are based on these BBBs should also be OK if they are properly designed and the

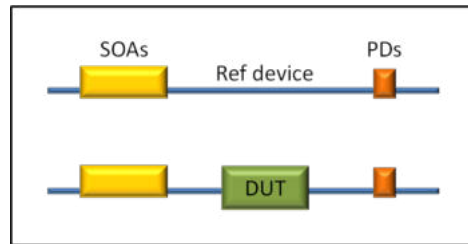


Figure 1.28: Measuring optical transmission of a DUT by comparing it to transmission through a reference device.

process is sufficiently mature. By restricting the testing to the basic building blocks, we avoid ending up with a large number of building blocks, the testing of which will require impractically large test cells. Also for process technology development it is practical to have a small set of basic building blocks, on which the process optimization can be focused.

1.9.2 On-Wafer Testing

Testing optical components is more difficult than testing electrical components. First, optical ports are only accessible after the wafer has been diced, and second the alignment tolerances for accurate coupling of light in or out of a waveguide are tight, so testing is slow. Alignment tolerances for electrical measurements are larger because the electrical contacts are larger and the effect of some misalignment is small as long as the contact is good. A great advantage of electrical measurements is that they can be done on-wafer: it is not necessary to dice the wafer for testing, which makes automated testing much easier.

In the PARADIGM project the possibilities for on-wafer testing of the optical properties of the most important building blocks in Photonic ICs have been investigated along two different tracks: one is by integrating vertical output couplers in the chip that can be accessed by vertical optical probes. The other approach is by integrating the Device Under Test (DUT) between sources and detectors that are integrated in the chip. In this latter approach we make use of the relative ease with which test circuits, even complex ones, can be added into ASPIC designs, and of the excellent wafer uniformity. We will describe this approach briefly in this section.

A general approach for measuring transmission loss is by comparing it to the transmission of a reference device, usually a straight waveguide section. We can do this on-wafer by integrating the DUT and the reference device between an integrated source and an integrated detector and measuring the transmission electrically by comparing the output currents of the detectors, under the assumption that the sources are identical. As a source we can use an integrated SOA section, which will generate a broad spectrum, so that the measured transmission will be averaged (weighted) over the full band. If we use an integrated DBR-laser as a source we can measure at a specific wavelength. The accuracy of the approach is dependent on the reproducibility of the integrated test sources and detectors.

The most important Basic Building Blocks are Passive Waveguide Devices, Semiconductor Optical Amplifiers and Phase Modulators. Their most important properties are propagation loss, gain spectrum and electro-optic efficiency, respectively. We will briefly describe generic structures for on-wafer testing of these components.

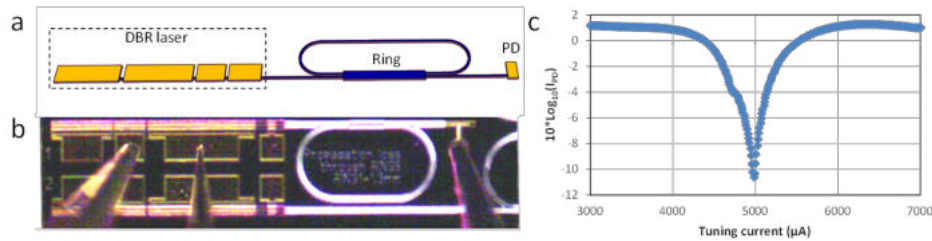


Figure 1.29: a) Schematic, b) microscope photo and c) measured response of a test structure for on-chip measurement of optical waveguide losses.

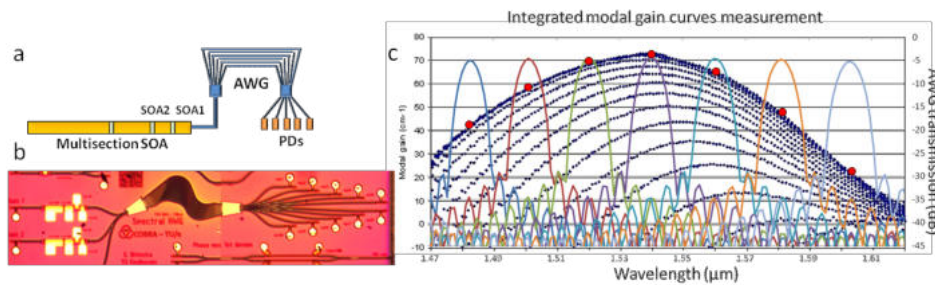


Figure 1.30: a) Schematic, b) microscope photo and c) sampling principle of a test structure for on-chip measurement of semiconductor optical amplifiers gain curves.

Waveguide losses can be measured, in principle, by comparing transmission through a short and a long waveguide section. If the propagation losses are low, a long waveguide section will be needed to measure the losses sufficiently accurately, and the test structure will have a large footprint. Another approach is shown in Figure 1.29. It is based on the fact that the transmission of ring resonators is very sensitive to the losses in the ring. For testing waveguide loss we insert a ring formed with an MMI-coupler between a tunable DBR laser with a monitor diode and a detector diode. By sweeping the wavelength and normalizing the detector current to the current of the monitor diode we record a curve as shown at the right of the figure. By measuring the extinction ratio between the maximum and minimum power we can determine the waveguide loss. For further increasing the measurement accuracy we can compare rings with the same curves but different lengths of the straight waveguide sections [95].

SOA Gain. Figure 1.30 illustrates a test structure for measuring the gain spectrum of an optical amplifier. If SOA1 and SOA2 are identical the ratio of the output power from SOA1 with SOA2 on and off is the gain of SOA1. The gain measured in this way is the weighted average over the gain spectrum. If we insert an AWG behind SOA1 and have photodetectors connected to each output port, we can measure the spectral gain for each wavelength channel of the AWG. This will give us a sampled gain spectrum as depicted by the red dots in Figure 1.30. A few channels will be sufficient for adequate validation of the SOA performance.

Electro-optic efficiency. A straightforward way to measure V_π , the voltage at which a phase modulator introduces 180° phase shift, is to insert it into a Mach-Zehnder Interferometer between an integrated source and detector, as depicted in Figure 1.31, and record the transmission as a function of the voltage. V_π is then the voltage difference between the two minima. In general it is voltage dependent, so a more sophisticated approach will be required to find the ϕ - V curve. Figure 1.31 illustrates the test struc-

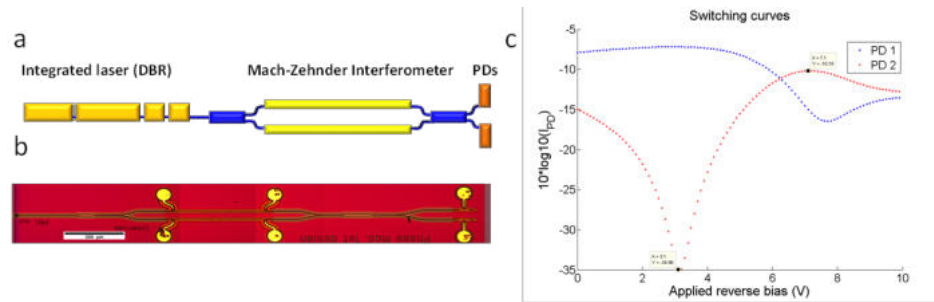


Figure 1.31: a) Schematic, b) microscope photo and c) measured response of a test structure for on-chip measurement of the electro-optic efficiency of a phase modulator.

ture.

The three examples illustrate how optical or electro-optical properties can be measured on-wafer using electrical probes. In Figure 2.103 the enlarged MPW cell appearing as an inset shows a test cell containing a number of test structures as described above. Such a test cell can be used for fast and accurate validation of the wafer, by measuring the performance of the Basic Building Blocks and comparing it to the specifications.

1.10 Conclusions

Generic InP-based foundry technology will lead to a dramatic reduction of the entry costs for companies that are interested in applying InP ASPICs in novel or improved products. It will bring advanced photonic InP-based integration technology within reach for many SMEs.

Major R&D funding by the EU and national governments has brought the foundry approach to a level that experimental foundry runs have been demonstrated successfully on industrial integration platforms, and semi-commercial access to the foundry platforms has started in 2013. Significant progress has been made in the development of process design kits and standardization of packaging and at present InP PDKs support significantly more powerful component libraries than silicon photonics. For small and medium volume production we expect InP to be very competitive indeed, since cost levels for participation in InP-based MPW runs are expected to be similar to those of advanced silicon photonics processes, while offering significantly more functionality.